

**GROUNDWATER ELEVATION ESTIMATION  
MODEL IN THE SLOPING OGALLALA AQUIFER**

by  
PHILIP G. MZAVA

B.S., University of Dar es Salaam, 2007

---

A THESIS

submitted in partial fulfillment of the requirements for the degree  
MASTER OF SCIENCE

Department of Civil Engineering  
College of Engineering

KANSAS STATE UNIVERSITY  
Manhattan, Kansas

2010

Approved by:

Major Professor  
David R. Steward

# Copyright

Philip G. Mzava

2010

# Abstract

A one-dimensional model was developed to study the flow of groundwater in the sloping Ogallala Aquifer at a steady state during predevelopment condition. The sloping base was approximated using a stepping base model. GIS applications were applied during data collection and preparation, and later during interpretation of model results. Analytical and numerical methods were employed in the development of this model which was used to try to understand long-term water balance in the study region. The conservation of mass was achieved by balancing groundwater input, output, and storage; this led to understanding the interactions of groundwater and surface water in the predevelopment conditions. The study resulted in identification of where natural discharge from groundwater to surface water occurred, and the quantity of these flows was obtained.

The Ogallala Aquifer is thick in the south western part of Kansas, this region had an average saturated thickness of 100m during predevelopment conditions. The model found that groundwater flowed at a discharge per width of approximately  $17 \text{ m}^2/\text{d}$  in this region. The aquifer thickness tends to gradually decrease from west to east and from south to north. The northern part had an average saturated thickness of 40m during predevelopment conditions; the model found that groundwater flowed at a discharge per width of approximately  $3 \text{ m}^2/\text{d}$  in this region. It was also found that groundwater leaves the Ogallala Aquifer on the eastern side with discharge per width between  $0\text{-}3 \text{ m}^2/\text{d}$ .

The discharge from groundwater to surface water was summed over contributing areas to river basins. The discharge to streams necessary to satisfy long-term conservation of mass computed by the model showed that Cimarron River has total baseflow of about  $5.5 \text{ m}^3/\text{s}$ ; this was found to be almost 100% of the total streamflow recorded during predevelopment conditions.

The Arkansas River was found to have total baseflow of about  $0.97 \text{ m}^3/\text{s}$ , which is approximately 14.3% of the total streamflow recorded during predevelopment conditions.

The Smoky Hill River was found to have total baseflow of about  $1.7 \text{ m}^3/\text{s}$ , which is approximately 73.9% of the total streamflow recorded during predevelopment conditions. The Solomon River was found to have total baseflow of about  $0.95 \text{ m}^3/\text{s}$ , which is approximately 41.1% of the total streamflow recorded during predevelopment conditions. The Saline River was found to have total baseflow of about  $0.25 \text{ m}^3/\text{s}$ , which is approximately 62.5% of the total streamflow recorded during predevelopment conditions. The Republican and Pawnee River was found to have total baseflow of about  $0.38 \text{ m}^3/\text{s}$  and  $0.22 \text{ m}^3/\text{s}$ , which is approximately 18.5% and 12.6% of the total streamflow in the predevelopment conditions respectively.

The model was found to be always within -16 to +12 meters between observed values and the model results, with an average value of 0.15m and a root mean square error of 1.98m. Results from this study can be used to advance this study to the next level by making a transient model that could be used as a predictive tool for groundwater response to water use in the study region.

# Table of Contents

Table of Contents	v
List of Figures	vii
List of Tables	viii
Acknowledgements	ix
Dedication	x
<b>1 Introduction</b>	<b>1</b>
1.1 Overview . . . . .	1
1.2 Organization of the report . . . . .	3
<b>2 Literature Review</b>	<b>4</b>
2.1 Ogallala Aquifer . . . . .	4
2.1.1 Geology . . . . .	7
2.2 Groundwater modeling . . . . .	8
2.2.1 Sloping bed drainage . . . . .	12
<b>3 Methods</b>	<b>15</b>
3.1 Analytical approach . . . . .	16
3.1.1 Basic equations . . . . .	16
3.1.2 The model . . . . .	18
3.2 Numerical approach . . . . .	21
<b>4 Application</b>	<b>23</b>
4.1 Model Results and Discussion . . . . .	24
<b>5 Conclusions</b>	<b>52</b>
<b>Bibliography</b>	<b>53</b>
<b>A GIS Procedures</b>	<b>58</b>
A.1 Projection . . . . .	58
A.2 Buffering . . . . .	59
A.3 Clipping . . . . .	60
A.4 Raster generation . . . . .	61
A.5 Unit conversion . . . . .	63

A.6	Permanent raster generation . . . . .	64
A.7	<i>Rename</i> and <i>point to raster</i> shortcuts . . . . .	65
A.8	Development of geodatabase for WIMAS data . . . . .	66
A.9	Batch Projection . . . . .	75
A.10	Spatial Interpolation-Inverse Distance Weighted . . . . .	76
A.11	Generation of rectangles using Python script . . . . .	77
<b>B</b>	<b>Computer program and Data input file</b>	<b>82</b>
B.1	Scilab script . . . . .	83
B.2	Sample data input file . . . . .	87
<b>C</b>	<b>Input data</b>	<b>88</b>

# List of Figures

1.1	Study area (Ogallala Aquifer in Kansas) . . . . .	2
2.1	High Plains Aquifer; showing the study region. . . . .	5
3.1	Conceptual model . . . . .	18
3.2	Program flowchart . . . . .	21
4.1	Estimated groundwater elevations at constant discharge per width of $1 \text{ m}^2/\text{d}$ . . . . .	25
4.2	Model accuracy at constant discharge per width of $1 \text{ m}^2/\text{d}$ . . . . .	26
4.3	Model result for cumulative recharge in the entire aquifer transect. . . . .	27
4.4	Potential groundwater-surface water interaction points. . . . .	28
4.5	Model result in the transect crossing Republican River. . . . .	30
4.6	Discharge graph for the transect crossing Republican River. . . . .	30
4.7	Model result in the transect crossing Cimarron River and Spring Creek. . . . .	31
4.8	Discharge graph for the transect crossing Cimarron River and Spring Creek. . . . .	31
4.9	Variations in discharge per unit width for the entire study region. . . . .	32
4.10	Unaccounted-for Baseflow. . . . .	33
4.11	Baseflow quantities at the groundwater-surface water interaction points. . . . .	34
4.12	Baseflow quantities in the Cimarron River Basin. . . . .	35
4.13	Baseflow quantities in the Arkansas River Basin. . . . .	35
4.14	Baseflow quantities in the Smoky Hill River Basin. . . . .	36
4.15	Baseflow quantities in the Solomon River Basin. . . . .	36
4.16	Baseflow quantities in the Republican River Basin. . . . .	37
4.17	Estimated groundwater elevations in the predevelopment conditions. . . . .	48
4.18	Model accuracy; difference between approximated and actual values of head. . . . .	49
4.19	Approximated depth to water in the predevelopment conditions. . . . .	50
C.1	Hydraulic conductivity . . . . .	88
C.2	Specific yield . . . . .	90
C.3	Predevelopment water level . . . . .	91
C.4	Surface elevation . . . . .	92
C.5	Annual potential recharge . . . . .	93
C.6	Bedrock elevation . . . . .	94

# List of Tables

2.1	Yearly total water withdrawal from Ogallala Aquifer, Kansas. . . . .	6
4.1	Cimarron River streamflow data. . . . .	38
4.2	Smoky Hill River streamflow data. . . . .	39
4.3	Arkansas River streamflow data. . . . .	40
4.4	Saline River streamflow data. . . . .	41
4.5	Solomon River streamflow data. . . . .	42
4.6	Beaver Creek streamflow data. . . . .	43
4.7	Republican River streamflow data. . . . .	44
4.8	Pawnee river streamflow data. . . . .	45
4.9	Approximate percentage of baseflow to the total streamflow. . . . .	47



# Acknowledgments

I would like to express my deepest gratitude and sincere thanks to my major advisor Dr. David R. Steward for giving me the opportunity to pursue Masters Degree at Kansas State University. I would also like to thank him for his continuous guidance through out my studies and in this research project.

I also grateful to NSF-EPSCoR at Kansas State Office for providing financial support for this research work, I would also like to thank my committee members Dr. Steven K. Starrett and Dr. Saugata Datta for accepting to provide supplemental advice, review my thesis, and supervise my Oral Examination.

Last but not least, I am truly thankful to all individuals who in one way or another were involved to make this study a success, my sincere thanks goes to Dr.Xiaoying Yang, and Richard Chubb for sharing their GIS expertise that helped a lot during this work.

# Dedication

*To Gabriel and Rose Mzava*

*My beloved parents*

# Chapter 1

## Introduction

### 1.1 Overview

Groundwater is an important source of fresh water supply. About 30% of all the fresh water on earth readily available for use is from underground storages (Aquifers). This amount is significant because much of the remaining 69% is found stored as ice in icecaps and glaciers, and it is not readily available for use. The remaining portion is characterized by surface water storages [*Hornberger, 1998*].

Groundwater flow and storage are continually changing in response to human and climatic stresses. Wise development of groundwater resources requires a more complete understanding of these changes in flow and storage and of their effects on the terrestrial environment and on numerous surface-water features and their biota [*Alley et al., 2002*].

Understanding of groundwater mechanics and its properties and availability is important. A number of studies have been done in the past to study this. For example, *Steward* [2007] examined the response of groundwater to changing water use practices in sloping aquifers. *Lawwo* [2007] examined how climate change affect groundwater level changes, and how does it subsequently affect the natural vegetation. This thesis builds upon the results from these particular studies.

This work studies steady one-dimensional groundwater flow in the sloping unconfined Ogallala Aquifer. The sloping base is approximated using the stepping base model. While trying to understand long-term water balance in the Ogallala Aquifer, this model is applied to simulate predevelopment groundwater conditions in the Ogallala Aquifer. The conservation of mass is achieved by balancing groundwater input, output (i.e recharge, baseflow), and storage. This leads to understand the interactions of groundwater and surface water in the entire Kansas portion of Ogallala Aquifer during predevelopment conditions. In particular, new knowledge is derived of where natural discharge from groundwater to surface water occurred, and the quantity of these flows.

This study focuses on western part of Kansas, which lies between Latitudes ( $37^{\circ} 06' 49.44''$  N,  $39^{\circ} 57' 48.22''$  N) and Longitudes ( $99^{\circ} 38' 51.78''$  W,  $102^{\circ} 04' 40.92''$  W), with the total area of approximately 5,898,940 hectares of Ogallala Aquifer in Kansas, covering 31 counties. See Figure 1.1 below.

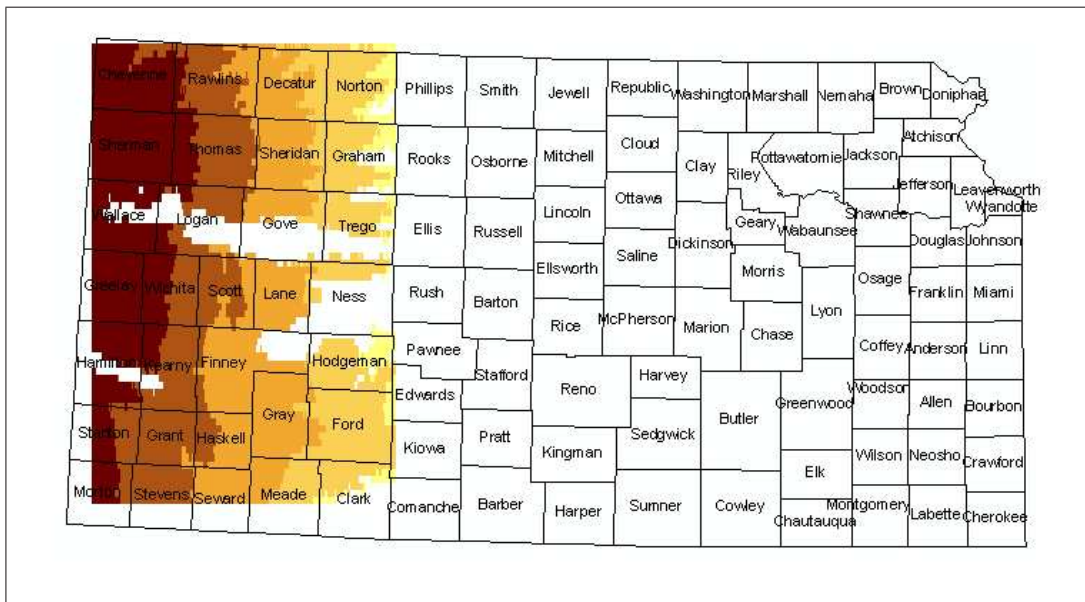


Figure 1.1: Study area (Ogallala Aquifer in Kansas)

The area has the highest surface elevation of 1203.2 meters on the west side to the lowest of 570.4 meters on the east side, and has a sloping base of approximately 0.23% from west to east. The Ogallala Aquifer covers approximately 89% of the study area, and it is the major source of groundwater in the region. The region obtains mean annual precipitation of between 16 and 24 inches, and mean annual potential natural recharge of between 0 and 2 inches (*Appendix C*) [Hansen, 1987]. This recharge data is the source of the groundwater discharges studied here.

## 1.2 Organization of the report

The present chapter gives an overview of the problem and the objective of this study, including why is the study important and what can be expected from it. It also gives the general information about the study region. The second chapter deals with a brief literature review on the study area, and the topic in question. The literature review presents the general information about Ogallala Aquifer, groundwater hydrology, and previous studies that have been done on groundwater modeling and sloping aquifers.

Chapter three of this report deals the Methodology. It covers in details about data preparation, the governing equations used to model groundwater and the specific equations used for this study. It also covers the Numerical approach, which includes coding with Scilab programming language. The fourth chapter presents model results and discussion. Lastly, Chapter five presents conclusions drawn from the results of this work. Relevant computer codes, figures, and tables are provided in the Appendices.

# Chapter 2

## Literature Review

### 2.1 Ogallala Aquifer

The most important component of the High Plains Aquifer is the Ogallala Aquifer, generally the western half of the High Plains aquifer in Kansas. The High Plains aquifer is a large (approximately 450,658 km<sup>2</sup> in portions of the eight states of South Dakota, Nebraska, Wyoming, Colorado, Kansas, Oklahoma, New Mexico, and Texas; with 86,765 km<sup>2</sup> of Kansas portion) body of sands, gravels, silts and clays (Fig. 2.1). It is regarded as one of world's largest aquifers. In western Kansas it is generally identical with the Ogallala formation, and the aquifer system was originally known as the Ogallala Aquifer. However, the part of the aquifer extending into south-central Kansas (east of Ford County) is now recognized as hydrologically similar but geologically different formations, and the combined aquifer system is referred to as the High Plains. The aquifer is now facing declining water levels and deteriorating water quality [*Buddemeier, 2000*].

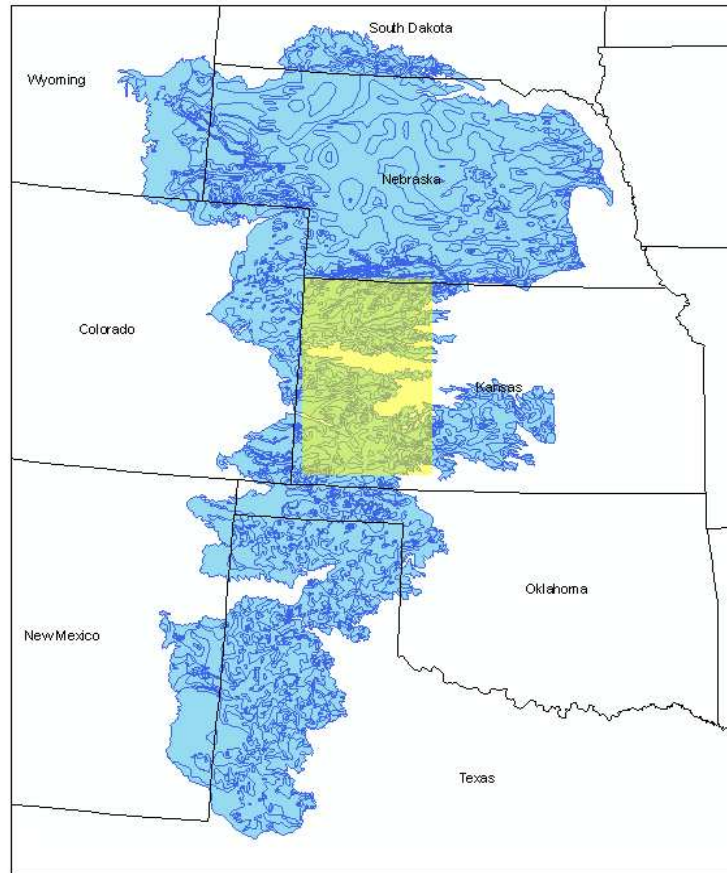


**Figure 2.1:** *High Plains Aquifer; showing the study region.*

Half of the U.S. population and almost all of those in rural areas draw water from underground aquifers for their domestic needs [Guru et al., 2000]. Additionally farmers depend on it for irrigation. Once thought an unlimited source of pure water, these sources are increasingly threatened. More than 90% of the water pumped from the Ogallala irrigates at least one fifth of all U.S. cropland [Guru et al., 2000]. About 27% of the irrigated land in the United States overlies this aquifer system, which yields about 30% of the nation's groundwater used for irrigation [Guru et al., 2000]. In addition, the aquifer system provides drinking water to 82 percent of the people who live within the aquifer boundary.

Crops that benefit from the aquifer are cotton, corn, alfalfa, soybeans, and wheat. These crops provide the Midwest cattle operations with enormous amounts of feed and account for 40% of the feedlot beef output here in the U.S. Since the advancement of agricultural irrigation in the earlier part of the 20th century, the Ogallala has made it possible so that states such as Nebraska and Kansas can produce large quantities of grain required to feed livestock [Guru et al., 2000].

Year	No. of Wells	Total Withdrawal (ac-ft)
1958	70	12,868.94
1959	769	197,601.73
1960	1,001	269,791.35
1961	1,015	277,031.11
1962	993	308,144.14
1963	1,129	403,437.06
1964	1,291	479,177.64
1965	1,333	387,098.52
1966	1,477	472,510.22
1967	1,376	475,034.85
1968	1,551	534,567.50
1969	1,737	480,554.05
1970	1,845	568,005.06
1971	1,950	626,867.45
1972	2,084	582,628.72
1973	2,295	640,504.96
1974	2,741	909,328.68
1975	2,960	966,878.75
1976	3,389	1,127,202.63
1977	4,161	1,218,219.66
1978	4,053	1,222,282.79
1979	4,291	1,152,335.80
1980	4,995	1,406,362.25
1981	19,273	4,852,650.49
1982	19,410	4,515,436.05

Year	No. of Wells	Total Withdrawal (ac-ft)
1983	19,343	4,129,719.90
1984	21,348	4,853,623.68
1985	20,733	4,214,205.25
1986	19,907	3,944,167.80
1987	21,463	4,103,381.53
1988	22,791	5,020,693.85
1989	25,004	4,750,501.57
1990	25,202	4,797,771.00
1991	25,585	4,940,827.12
1992	24,081	3,589,503.71
1993	22,931	3,150,607.90
1994	25,059	4,181,553.85
1995	24,708	3,861,634.02
1996	24,960	3,600,033.55
1997	25,268	3,478,354.56
1998	25,320	3,739,144.87
1999	25,437	3,441,236.82
2000	25,592	4,194,304.56
2001	25,653	3,873,516.45
2002	26,036	4,552,514.85
2003	26,028	4,027,743.24
2004	25,630	3,447,740.56
2005	25,619	3,259,206.30
2006	25,614	3,791,643.78

**Table 2.1:** Yearly total water withdrawal from Ogallala Aquifer, Kansas.



### 2.1.1 Geology

Aquifer characteristics are determined in large part by geology. The High Plains aquifer is composed mainly of silt, sand, gravel, and clay-rock debris that washed off the face of the Rocky Mountains and other more local sources over the past several million years. The aquifer varies greatly from place to place: thick in some places, thin in others; permeable (able to transmit water easily) in some places, less so in others. Where the deposits are thick and permeable, water is easily removed and the aquifer can support large volumes of pumping for long periods. In most areas, this water is of good quality. In some locations (such as Lake Scott State Park in Scott County), the Ogallala Formation crops out at the surface, forming a naturally cemented rock layer called mortarbeds. In the subsurface, the Ogallala largely consists of silt and clay beds that are interlayered with sand and gravel that is mostly unconsolidated, or not naturally cemented together.

The south-central extension of the High Plains aquifer is composed of younger sediments that are similar to the Ogallala. These younger sediments, deposited during the Pleistocene Epoch, or Ice Ages, include the “Equus beds” aquifer (in McPherson, Reno, Harvey, and Sedgwick counties) and the “Great Bend Prairie aquifer” (in Stafford, Edwards, Pratt, Kiowa, and other counties). Also lying above the Ogallala Formation are other Pleistocene deposits and other younger deposits in the valleys of modern streams. Where these stream deposits (known as alluvium) are connected to the Ogallala or Pleistocene aquifers, the alluvial aquifers are considered part of the High Plains Aquifer [*Buchanan, 2001*].

Hydraulic conductivity and specific yield are highly variable because of the heterogeneity of the aquifer. Hydraulic conductivity and specific yield of the aquifer depend on sediment types, which vary significantly both horizontally and vertically. Hydraulic conductivity ranges from less than 25 to greater than 300 feet per day, with an average of 60 feet per day. Specific yield ranges from less than 10 to about 30 percent and averaging 15 percent [*Gutentag et al., 1984*].

## 2.2 Groundwater modeling

A model is a tool designed to represent a simplified version of reality. Groundwater models are also representations of reality and, if properly constructed, can be valuable predictive tools. The validity or reliability of the predictions will depend on how well the model approximates field conditions. Good field data are essential when using a model for predictive purposes. However, an attempt to model a system with inadequate field data can also be instructive as it may serve to identify those areas where detailed field data are critical to the success of the model. In this way, a model can help guide data collection activities.

Several types of models have been used to study groundwater flow systems, they can be divided into three broad categories (*Prickett, 1975*): *sand tank models*, *analog models* - including viscous fluid models and electrical models, and *mathematical models* - including analytical and numerical models. A mathematical model consists of a set of differential equations that are known to govern the flow of groundwater. Mathematical models of groundwater flow have been in use since the late 1800s. Simplifying assumptions must always be made in order to construct a model because the field situations are too complicated to be simulated exactly. Usually the assumptions necessary to solve a mathematical model analytically are fairly restrictive. For example, many analytical solutions require that the medium be homogeneous and isotropic. To deal with more realistic situations, it is usually necessary to solve the mathematical model approximately using numerical techniques. Since the 1960s, when high-speed digital computers became widely available, numerical models have been the favored type of model for studying groundwater [*Wang et al., 1982*].

Groundwater flow models have a long history and come in many forms. Finite-difference and finite-element methods are presently the most common numerical techniques for modeling groundwater flow. Early flow models were based primarily on the finite-difference method of approximation of the governing field equations. Simple in concept and computationally efficient, finite-difference models found broad acceptance by the groundwater community. Later model development focused on the finite-element approach, which was

more mathematically abstract and more difficult to code. The finite-element approach had the advantage of being able to represent irregular aquifer geometries more accurately because unlike the broadly used version of the finite-difference model which relied on rectangular meshes. Finite-element models could accommodate triangular and even deformed rectangular meshes. Both finite-difference and finite-element models are currently used routinely in groundwater hydrology and groundwater-contaminant hydrology to predict groundwater-reservoir behavior [*Pinder, 2002*].

The Analytic Element Method is another numerical method used for the solution of partial differential equations. It is most often applied to problems of groundwater flow governed by the Poisson equation, though it is applicable to a variety of linear partial differential equations, including the Laplace, Helmholtz, and biharmonic equations. This method was initially developed by O.D.L. Strack at the University of Minnesota. The basic premise of the analytic element method is that, for linear differential equations, elementary solutions may be superimposed to obtain more complex solutions. A suite of 2D and 3D analytic solutions (“elements”) are available for different governing equations. These elements typically correspond to a discontinuity in the dependent variable or its gradient along a geometric boundary (e.g., point, line, ellipse, circle, sphere, etc.). This discontinuity has a specific functional form (usually a polynomial in 2D) and may be manipulated to satisfy Dirichlet, Neumann, or Robin (mixed) boundary conditions.

Each analytic solution is infinite in space and/or time. In addition, each analytic solution contains degrees of freedom (coefficients) that may be calculated to meet proscribed boundary conditions along the element’s border. To obtain a global solution (i.e., the correct element coefficients), a system of equations is solved such that the boundary conditions are satisfied along all of the elements (using collocation, least-squares minimization, or a similar approach). Notably, the global solution provides a spatially continuous description of the dependent variable everywhere in the infinite domain, and the governing equation is satisfied everywhere exactly except along the border of the element, where the governing equation is

not strictly applicable due to the discontinuity [*Wikipedia*, the online free encyclopedia].

The difference between the analytic element method and the finite-difference, and finite-element methods are; in the finite-difference and finite-element methods, the potential is approximated by discretization throughout the flow domain. As a result, not only the boundary conditions are approximated, but also the differential equation itself. The analytic element method does not rely upon discretization of volumes or areas in the modeled system, only internal and external boundaries are discretized. Characteristic for both the finite-difference and finite-element methods is that the flow domain is bounded, in contrast to the analytic element method where the aquifer system is modeled as being infinite in extent; boundary conditions are applied only along internal boundaries that are physically present in the aquifer system. Advantages of both the finite-difference and finite-element methods are that the hydraulic conductivity can be easily varied (e.g. from node to node) throughout the aquifer system, that the formulations are suitable for modeling transient flow, and that they are comparatively straight-forward [*Strack*, 1989].

A paper on the application of the analytic element method was presented by *Hunt* [2006]. This paper points out the overview of the applications of this method in comparison to other methods like finite-difference or finite element methods. This paper list the historic applications of the AEM as it has been used in regional, two dimension steady state models, analyses of groundwater-surface water interaction, quick analyses and screening models, wellhead protection studies. Others were grid sensitivity analysis, estimating effective conductivity and dispersion in highly heterogeneous systems. This paper also point out where more method development is needed in AEM including a three-dimensional and transient simulation [*Hunt*, 2006].

By using analytic elements to model steady state, two-dimensional, Dupuit-Forchheimer groundwater flow and its contribution to surface flow, average base flows and groundwater flows in a groundwater and surface water system can be model without substantial increase in model complexity or data requirement. [*Haitjema*, 1996]. Analytic element method used

for modeling of divergence-free and irrotational flow in both two and three dimensions, including the description of the superblock approach which makes it possible to deal with very large models both in terms of accuracy and speed, solving multiaquifer problems was presented by *Strack* [2003].

Groundwater and surface water interaction of the Northern Highland Lakes region of Wisconsin, USA were examined by using remote sensing, and AEM. The remote sensed elevation data for lakes and wetlands were used to construct regional scale groundwater models. The Elevation data were then utilized in ArcAEM to perform the groundwater model development for Wisconsin area [*Fredrick et al., 2006*].

The analytic element method can be used to examine groundwater flow in multiaquifer system. Differential equations are developed based on AEM and each equation represent a physical feature such as well, line-sink, and circular infiltration. Solution to these equations can be used to simulate results for the aquifer head, discharge and leakage between aquifers at any point. If these AEM differential equations are superimposed, a solution to a regional multiaquifer flow can be simulated. The analytic element method is a prominent technique used for modeling local detail within a large regional system [*Bakker et al., 2002*].

New technique to further improve modeling efforts involve the integration of groundwater modeling with geographical information systems (GIS). Introduction of GIS in groundwater modeling stems from the realization that from the outset, groundwater modeling has entailed the organization, quantification, and interpretation of large quantities of geohydrological data. Early work in groundwater modeling required the translation and transfer of information on maps, charts, and tables into computer-readable form. The work was lengthy, tedious, and error prone.

Changes that were required in the data sets in the course of calibrating the models often involved sifting through thousands of numbers to make what often turned out to be minor modifications to the input-data sets. The specification of hydrological information such as rainfall, parametric information such as hydraulic conductivity, design parameter

specifications such as well locations and discharge values, and auxiliary conditions such as boundary conditions all involve the organization and manipulation of enormous quantities of data. Virtually all of this information is spatially, and in some instances temporally, distributed. Much of it is available in computerized databases either as maps in bitmap or vector image format or as data tables. Due to advances in computer-graphical technology, the information in such databases is now accessed most efficiently through GIS systems [Pinder, 2002].

An object oriented approach that associate groundwater models based on analytic element method with GIS geodatabase features that uses AEM model interface can be developed to establish a link between groundwater to a variety of natural and social process [Steward et. al, 2006].

### 2.2.1 Sloping bed drainage

The approximation analysis of the flow of groundwater resting on an impermeable bed initiated by *Dupuit* [1863] and continued by *Boussinesq* [1904] has received renewed attention in recent years, directed more particularly to the situation in which the bed is sloping. The essence of the approximation as it relates to a horizontal bed is that when the lateral extent of the aquifer is very large compared with its thickness, the flow must necessarily be constrained to directions that are parallel to the bed and therefore horizontal. It follows that the equipotentials are parallel vertical planes and that therefore the potential gradient and the flow are uniform throughout the vertical section. Moreover, each equipotential is labeled from the fact that it intersects the water table at a known height relative to the bed, which may therefore be taken as the potential throughout the section. The potential gradient is then simply the slope of the water table at the intersection with the equipotential. By means of Darcy's law one may then express the total flow across a unit width of the equipotential plane in terms of the slope of the water table and the water table height above the bed [Childs, 1971].

Unconfined groundwater flow in a sloping aquifer may be modeled using the nonlinear Boussinesq equation, based on the classical Dupuit approximation. Solutions of such an equation are of interest in groundwater catchment hydrology, coastal groundwater hydraulics, and several other nonlinear diffusion problems. [Daly et al., 2004]. *Daly* studied particular cases of groundwater flow along a hillslope using the groundwater hydraulic theory (e.g. Dupuit approximation) described by the Boussinesq equation. Analytical solutions were found as simple transformations of known similarity solutions. The study presented some analytical solutions of the Boussinesq equation describing the groundwater flow along a hillslope. By means of a simple travelling wave coordinate transformation, the Boussinesq equation is written as if the flow occurred on a horizontal impermeable bed, for which exact similarity solutions are well known. The practical applicability of the approach is somewhat limited by the fact that the same transformation must also apply to the initial and boundary conditions; however, the analysis may be useful to clarify some mathematical and physical aspects of the problem and to furnish benchmarks for the validation of numerical simulations.

*Steward* et al. [2009] examined the impact of a sloping base on the movement of transients through groundwater systems. Dimensionless variables and regression of model results were employed to develop functions relating the transient change in saturated thickness to the distance upgradient and downgradient from recharge or withdrawal. Convolution of these transient response functions enabled computation of changes in saturated thickness over recharge or withdrawal that varied over space and time.

Solutions for steady and transient flow using physical and numerical models for recharge-induced groundwater flow over a sloping bed, was studied by *Chapman* [2005]. The study looked at the free surface profile and outflow hydrograph for groundwater under conditions of steady uniform recharge followed by recession in viscous fluid model test, using a sloping bed with a gradient of 0.2. The data was compared with the nonlinear Boussinesq model and a modification of that model simulating the outflow seepage surface, obtained from a

finite difference solution of the free boundary problem.

*Steward* [2007] examined groundwater flow for recharge and extraction within a sloping aquifer. Fundamental equations were formulated in commonly used coordinates systems;  $s-n$  and  $x-z$  coordinates. Consistency between these two formulations was achieved by incorporating the slope of the base directly into the hydraulic conductivity and aquifer diffusivity terms. A stepping model was developed for steady and transient flow, and it was then compared to sloping model and exact solutions. A set of nomographs and dimensionless parameters relating drawdown over time to distance upgradient, or downgradient from a point of water use was developed from the model.



# Chapter 3

## Methods

This chapter describes in detail the methods that were used in this study. Analytical and Numerical modeling approaches were employed during the modeling work in this study. The mathematical equations are derived from basic groundwater flow equations, and the equations were implemented using Scilab computer programming language. The first step was data collection and preparation; data that was collected for the purpose of this work include: hydraulic conductivity, specific yield, bedrock elevation, surface elevation, predevelopment water levels, water use, recharge, and Kansas map showing state and county boundary lines.

After data collection, ArcGIS software was used during data preparation to transform the data to a format that was useful for the numerical modeling. Step by step description of data preparation is found in *Appendix A* of this report. Briefly, the following procedure was followed during data preparation after the data was collected: data projection, buffering, clipping, WIMAS water use data extraction, raster generation and unit conversion, generation of rectangles, and transformation of data to CSV format.

Water use data requested from WIMAS came in Microsoft Access format, and so it had to be processed to be consistent with other data which were either in vector or raster format, this process is also discussed in *Appendix A*. After the process of raster generation and unit conversion, the raster data had cell size of 100 x 100 meters. Since the original data came in different form e.g. polygons, polylines, points etc., this procedure was necessary so as to have consistency in representation of all the data models, which made them easy to work

with. Then the raster data had to be transformed back to shapefiles so as to be able to extract the data from the raster format, only this time they will all be in one consistent format. This is where the generation of rectangles process was carried out.

1km x 5km rectangles (shapefiles) were generated which contained mean values of all the 100 x 100 meter raster cells contained in them, this was done for all the data mentioned above. The last procedure of data preparation was to export the data from ArcGIS (Attribute tables) and save them as comma separated text files (CSV) (*Appendix B*). A Scilab script written to implement the groundwater flow equations used for this study read the input data/variables from this CSV file. The model was then run and calibrated to match the measured/actual conditions, and the interpretation of the model results was done at last.

## 3.1 Analytical approach

### 3.1.1 Basic equations

The theory of groundwater flow is based on a law first discovered by Darcy in 1856 (3.1). Darcy's law is an empirical relation for the specific discharge in terms of the head ( $\phi$ ).

$$q_i = -k \frac{\partial \phi}{\partial i} \quad (i = x, y) \quad (3.1)$$

Combining the Dupuit assumption (3.2); that head does not vary in the  $z$ -direction perpendicular to the base, and Darcy's law, provides a simpler way to deal with both unconfined and confined conditions of groundwater flow with discharge per unit width  $Q_i$  (3.3). This is by introduction of new variable,  $\Phi$ , referred to as *discharge potential*, with the assumption of constant hydraulic conductivity ( $k$ ), bedrock elevation ( $B$ ), and saturated thickness ( $H, \phi - B$ ).

$$Q_i = \begin{cases} q_i(\phi - B) & (\phi - B) < H \\ q_i H & (\phi - B) \geq H \end{cases} \quad (3.2)$$

$$Q_i = -\frac{\partial \Phi}{\partial i} \quad (3.3)$$

The governing equation (3.5) is found by combining equation 3.3 with the equation of conservation of mass (3.4).

$$\frac{\partial Q_x}{\partial x} + \frac{\partial Q_y}{\partial y} = R - S \frac{\partial \phi}{\partial t} \quad (3.4)$$

Problems of groundwater flow can be solved by determining a function  $\Phi$  that fulfills equation 3.5 and satisfies the boundary conditions.

$$\frac{\partial^2 \Phi}{\partial x^2} + \frac{\partial^2 \Phi}{\partial y^2} = -R + \frac{1}{\alpha} \frac{\partial \Phi}{\partial t} \quad (3.5)$$

Where  $R$  is recharge and  $\alpha$  is aquifer diffusivity.

For unconfined and confined conditions of groundwater flow, the potential  $\Phi$  and head  $\phi$  are related as [Strack, 1989]

$$\Phi = \begin{cases} \frac{1}{2}k(\phi - B)^2 & (\phi - B) < H \\ kH(\phi - B) - \frac{1}{2}kH^2 & (\phi - B) \geq H \end{cases} \quad (3.6)$$

### 3.1.2 The model

This section demonstrates how the steady one-dimensional groundwater flow model in an unconfined aquifer with a sloping base was developed using a stepping base approach. Basic equations described above were used to come up with specific solution to the problem. The conceptual model (Fig. 3.1) shows the variables that were used to produce the actual model.

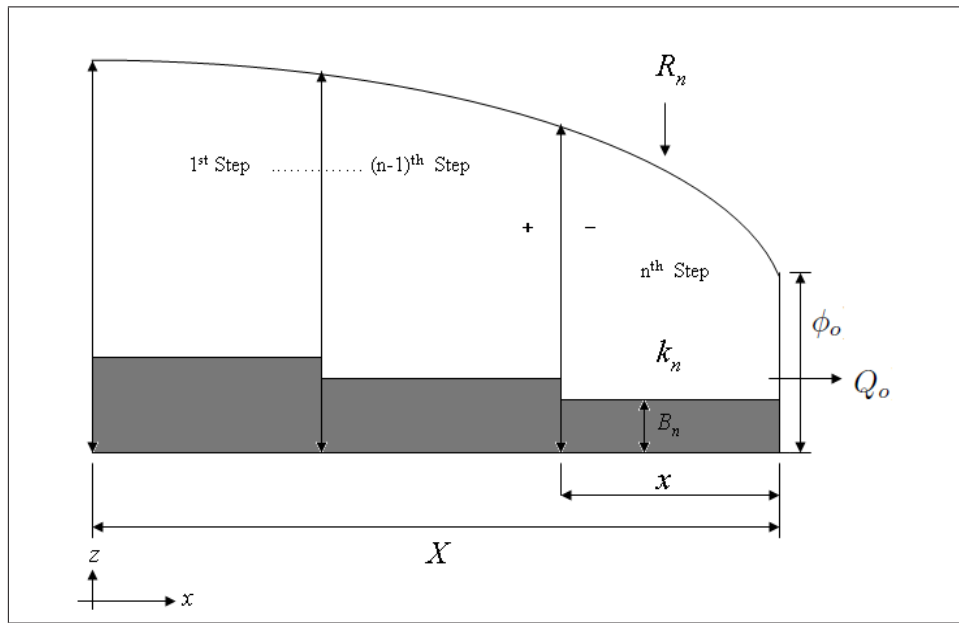


**Figure 3.1:** *Conceptual model*

Since this study only deals with a steady state one-dimensional model, the governing equation (3.5) is reduced to

$$\frac{\partial^2 \Phi}{\partial x^2} = -R \quad (3.7)$$

The function  $\Phi$  (3.8) that fulfills equation 3.7 and satisfies the boundary conditions provides solution to this steady one-dimensional groundwater flow problem in an unconfined sloping aquifer using stepping base approach

$$\Phi = -\frac{R}{2}x^2 - Q_o x + \Phi_o \quad (3.8)$$

The groundwater levels were estimated by starting with known value of head ( $\phi_o$ ), and specified value of discharge per unit width ( $Q_o$ ) at the far right end (Fig. 3.1). Then the proceeding values of head from right to left were estimated in step-wise approach over segments with uniform properties i.e. hydraulic conductivity ( $k$ ), bedrock elevation ( $B$ ), and recharge ( $R$ ).

Since this study deals with unconfined aquifer conditions, from 3.6, transformation of head to potential was done using

$$\Phi_o = \frac{1}{2}k_n(\phi_o - B_n)^2 \quad (3.9)$$

Where  $\phi_o$  is the starting head on the right hand side of each segment, starting with the known head at the far right end.  $k_n$  and  $B_n$  are hydraulic conductivity and bedrock elevation for the  $n$ th segment respectively. Equation 3.8 was used to obtain consecutive potentials from right to left.

$$\Phi = -\frac{R_n}{2}(X_i - X_{i+1})^2 - Q_o(X_i - X_{i+1}) + \Phi_o \quad (3.10)$$

Where  $R_n$  is the recharge rate for the  $n$ th segment, an index  $i$  was used to obtain the length ( $x$ ) of segments with uniform properties from the total transect length ( $X$ ).  $Q_o$  is the starting discharge per unit width on the right hand side of each segment, starting with a specified discharge per unit width at the far right end.

From equation 3.3, it can be seen that discharge per unit width does not remain constant in this case. Therefore the change in discharge per unit width was obtained using

$$Q_x = -\frac{\partial\Phi}{\partial x} = R_n(X_i - X_{i+1}) + Q_o \quad (3.11)$$

Equation 3.9 can be written in a different way to calculate head for different values of potential obtained from equation 3.10

$$\phi = B_n + \sqrt{\frac{2\Phi}{k_n}} \quad (3.12)$$

To ensure continuity of flow and no jumps in head at the interface; where the aquifer properties are changing, conditions specified in equation 3.13 had to be satisfied when looking for the solution.

i.e. *at the interface*:

$$\begin{aligned} \phi^+ &= \phi^- = \phi_o \\ Q_x^+ &= Q_x^- = Q_o \end{aligned} \quad (3.13)$$

To satisfy the above conditions, the last calculated head and discharge to the left of the *n*th segment was considered the starting head and discharge at the right hand side of the *n-1* segment. This process goes on for approximation of groundwater levels for the entire aquifer transect.

## 3.2 Numerical approach

Computer application for implementation of mathematical equations described in the analytical approach section was unavoidable. This is because of large extent of study area which resulted to large quantity of data to be processed. This approach provides a convenient way to obtain, visualize, and analyze results. The mathematical equations were coded using Scilab programming language, the following is the flowchart representing the code (*Appendix B*) structure.

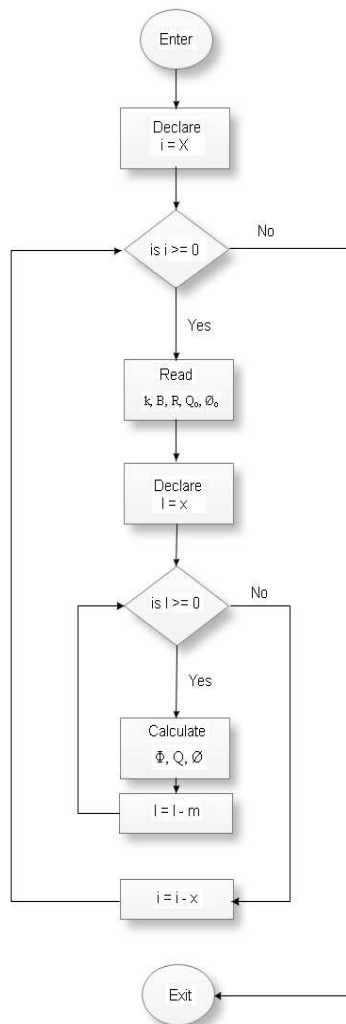


Figure 3.2: Program flowchart

The code is made of two nested for-loops. The inner loop is used for calculation of groundwater elevations ( $\phi$ ) and discharges ( $Q_x$ ) for steps with uniform properties i.e.  $k$ ,  $B$  and  $R$ . The outer loop is used to move from one step to the next. Both loops are controlled by distances  $x$  and  $X$ ; the length of steps with uniform properties and the length of entire aquifer transect respectively. Figures 3.1 and 3.2 explain the program in greater details.



# Chapter 4

## Application

This chapter deals with the outputs obtained after application of methods discussed in the previous chapter. The results are displayed and discussed for different scenarios.

The data that was used in this study was obtained from the following sources:

1. Kansas boundary lines [*U.S. Census Bureau*]  
<http://www.kansasgis.org>
2. Hydraulic conductivity [*Gutentag et al., 1984*]  
<http://water.usgs.gov/lookup/getgislist>
3. Specific yield [*Gutentag et al., 1984*]  
<http://water.usgs.gov/lookup/getgislist>
4. Predevelopment water levels [*Gutentag et al., 1984*]  
<http://water.usgs.gov/lookup/getgislist>
5. Bedrock elevation [*Gutentag et al., 1984*]  
<http://water.usgs.gov/lookup/getgislist>

6. Water use [*WIMAS, Kansas Geological Survey*]

<http://www.kgs.ku.edu>

7. Surface elevation [*U.S. Geological Survey*]

<http://www.kansasgis.org>

8. Recharge [*Hansen, 1987*]

More information on the data listed above is found in *Appendix C*.

## 4.1 Model Results and Discussion

The aquifer geometry was obtained using GIS applications discussed in *Appendix A*. Briefly, after generation of the data rectangles, intersection of these rectangles with the digital map of the High Plains Aquifer boundary, Kansas State and County boundary lines was done to obtain the portion of Ogallala Aquifer displayed here. The boundary conditions applied to obtain the results discussed in this section are: known values of predevelopment groundwater elevation and a specified discharge at the far right-hand boundary of the Ogallala Aquifer.

A constant discharge (no recharge) scenario was first used to test the model, the model produced results (Fig. 4.1) with similar pattern to predevelopment conditions. The Ogallala Aquifer decrease in thickness from West to East, and also from South to North, it was difficult with this approach to find an optimal value of discharge that would produce close approximation of groundwater elevations in the regions with thick aquifer saturated thickness without over estimation in the regions with thin aquifer saturated thickness, and vice versa. This is because the constant discharge approach is not realistic.

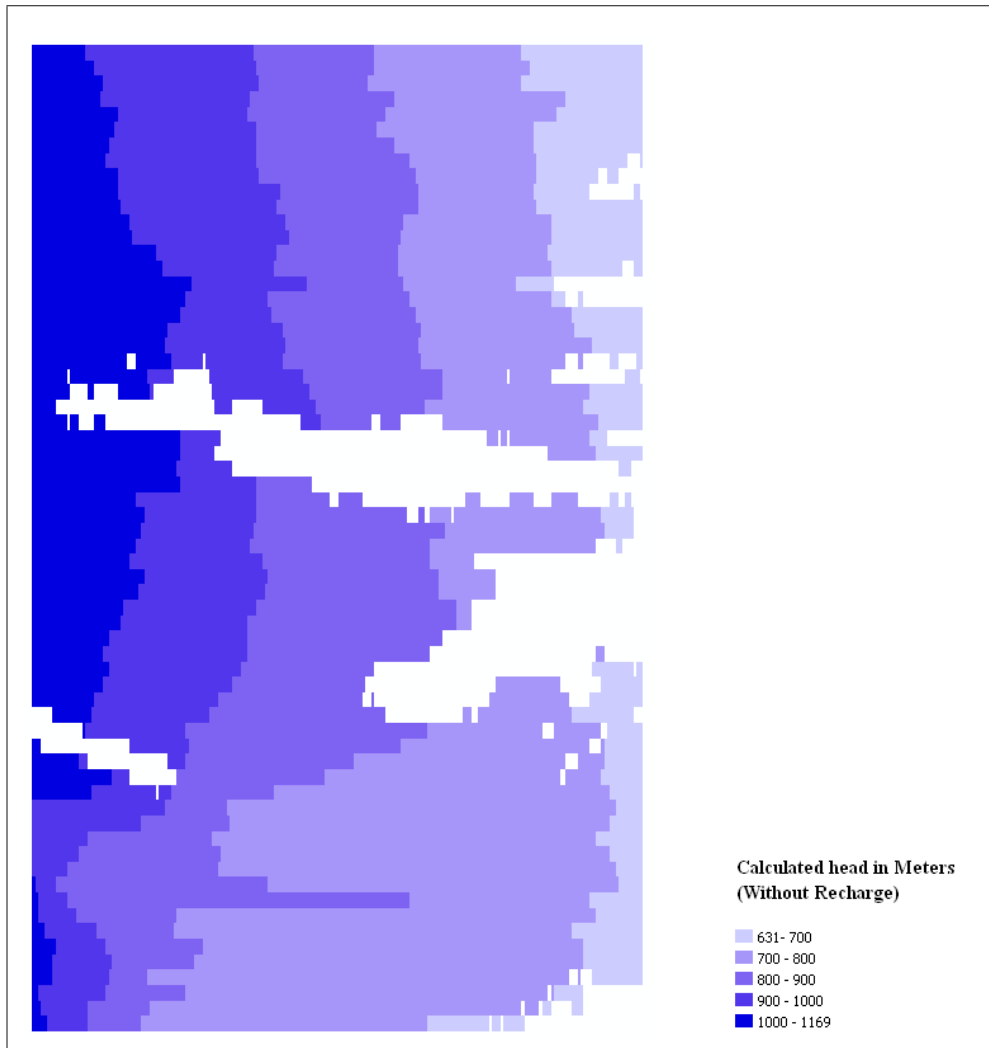


**Figure 4.1:** *Estimated groundwater elevations at constant discharge per width of  $1 \text{ m}^2/\text{d}$ .*

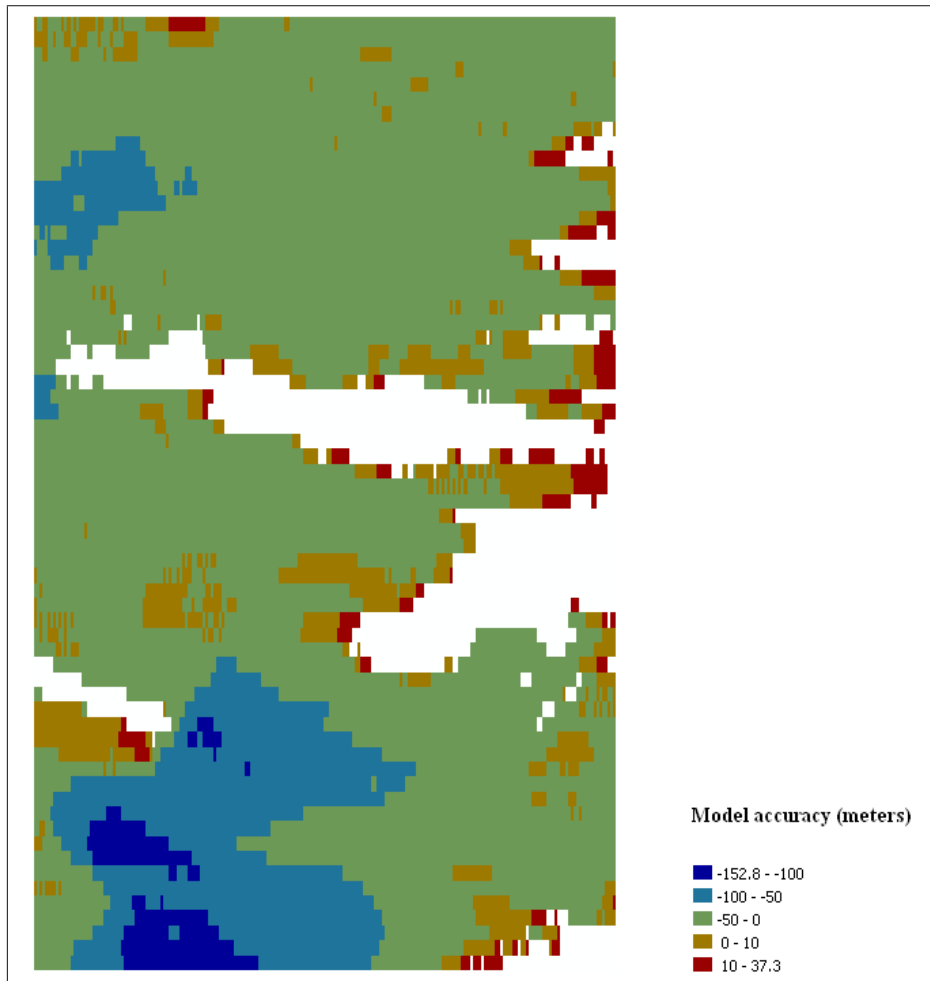


**Figure 4.2:** *Model accuracy at constant discharge per width of  $1 \text{ m}^2/\text{d}$ .*

Figure 4.2 shows the difference between the actual and calculated groundwater elevations using the constant discharge approach at an optimal discharge per width of  $1 \text{ m}^2/\text{d}$ . It can be observed that the model results had lower error on the eastern side where water leaves the aquifer, and the error increased consistently to the west. This is because the model starts the approximation from the east where the aquifer is thin and therefore thin saturated thickness, and continue to the west where the aquifer have thick saturated thickness which was impossible to compensate using this approach. Although this was not a realistic approach, it showed that the model was working. It also showed that there are variations in discharge in the aquifer which need to be studied further.

A more realistic approach was done next, which incorporated recharge in the model. Since water moves from higher elevation (west) to lower elevation (east), and the model works from east to west, the first trial was done by starting with a discharge at the far right hand (boundary condition) that accounts for all the recharge that happened in the aquifer entirely from left to right. This was by assuming that all the recharged water exit the aquifer at the furthest eastern point.

Results along a west-east transect towards the north-most portion of the Ogallala is shown in figure 4.3, these results did not match the actual conditions. It is true that all that water had infiltrated the aquifer, and according to the law of conservation of mass, a water balance has to be achieved in the system. From the results obtained here, it was obvious that the balance could not be found by only taking water out at the furthest eastern point; instead, there are more than one point where groundwater is discharging to the surface water.

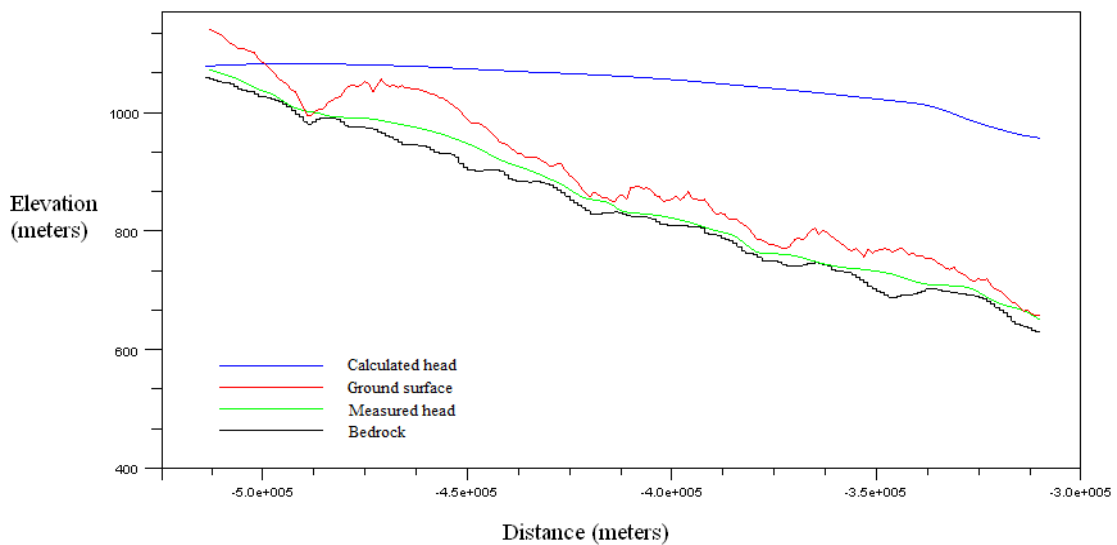


**Figure 4.3:** *Model result for cumulative recharge in the entire aquifer transect.*

A method to find points for taking water out was devised so as to try to simulate pre-development conditions, and by doing so, achieving the law of conservation of mass. Points

within the study region which are  $\pm 6\text{m}$  from the ground surface where determined and colored red in figure 4.4. These were considered potential points where groundwater can interact with the surface. These points were used when necessary to take water out at a rate sufficient enough to produce close approximation of groundwater elevations on the up-gradient side.

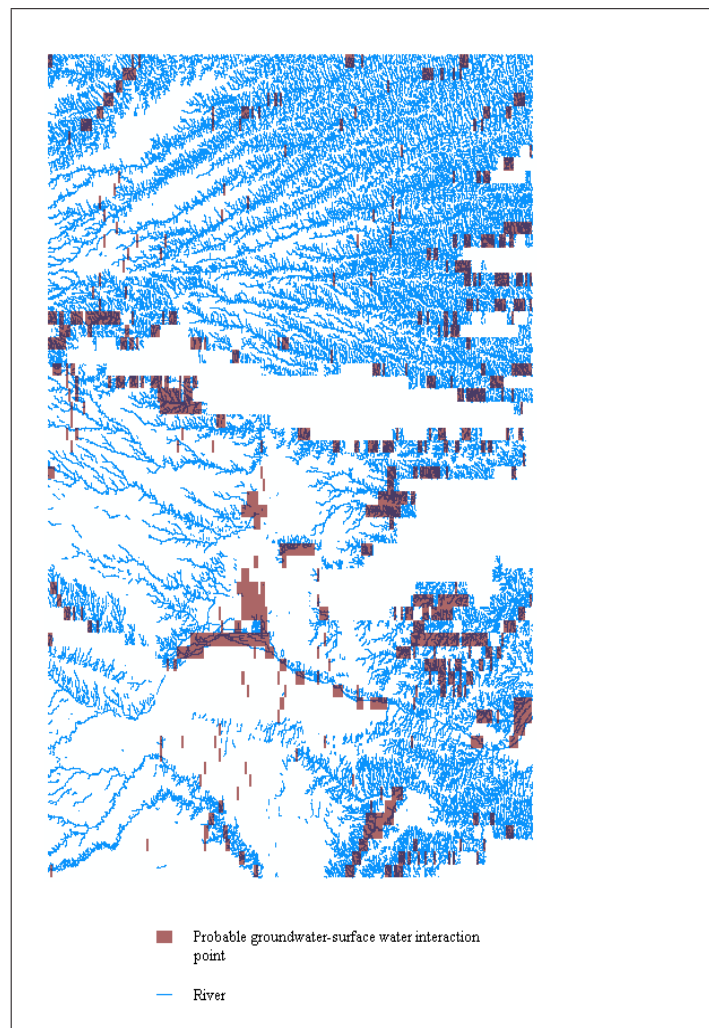


**Figure 4.4:** *Potential groundwater-surface water interaction points.*

A trial and error method was devised to determine the discharges to remove from these cells together with the help of equation 4.1 [Steward, 2007]. This equation relates the

discharge per width ( $Q_x$ ) to the saturated thickness (D) in the aquifer with uniform base slope using

$$Q_x = -kD\left(\frac{\partial D}{\partial x} + \tan\theta\right) \quad (4.1)$$

where k is the hydraulic conductivity and  $\theta$  is the angle of the sloping base.

At normal depth  $\frac{\partial D}{\partial x} = 0$  ; since groundwater tends to try to flow at normal depth, therefore

$$Q_{xo} = -kD_o \tan\theta \quad (4.2)$$

With known value of normal depth ( $D_o$ ) that is happening up-gradient, equation 4.2 was used to calculate discharge at normal depth ( $Q_{xo}$ ) which happens up-gradient for segments with constant slope. Since this equation does not incorporate recharge, it was only used to give a rough estimate of a minimal discharge that could be happening at the point of water out-take in the down-gradient side. Thereafter, with the ability to visualize and compare results, a trial and error method was used to approximate groundwater elevations to the nearest meters by taking enough water out to achieve mass balance.

The following figures show some of the model results after accomplishing mass balance to best approximate groundwater elevations, and simulate predevelopment conditions. The groundwater elevation and discharge is shown in figures 4.5 and 4.6 respectively along a transect in the northern portion of the Ogallala. Figures 4.7 and 4.8 show groundwater elevation and discharge respectively along a transect in the southern portion of the Ogallala.

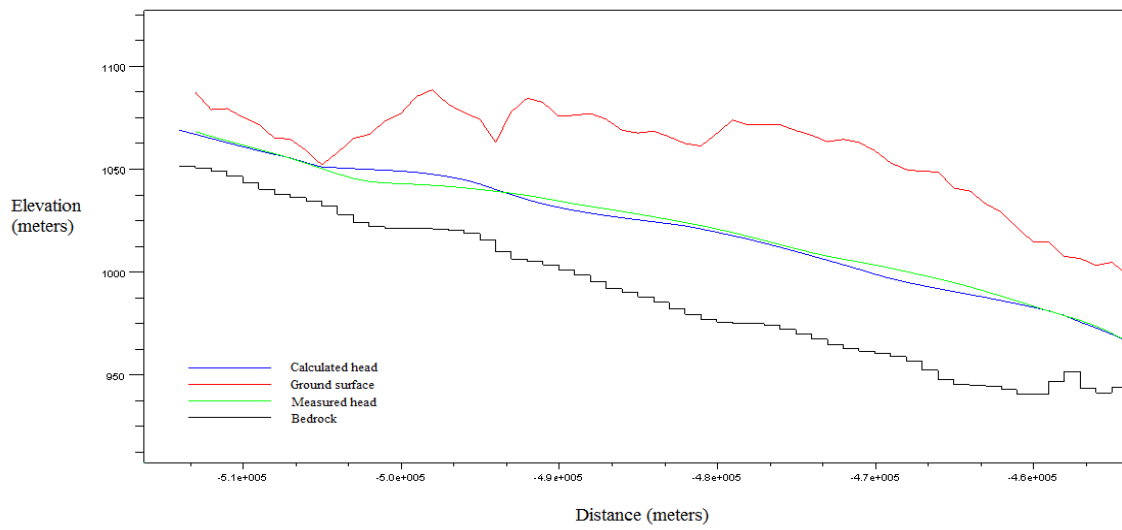


Figure 4.5: Model result in the transect crossing Republican River.

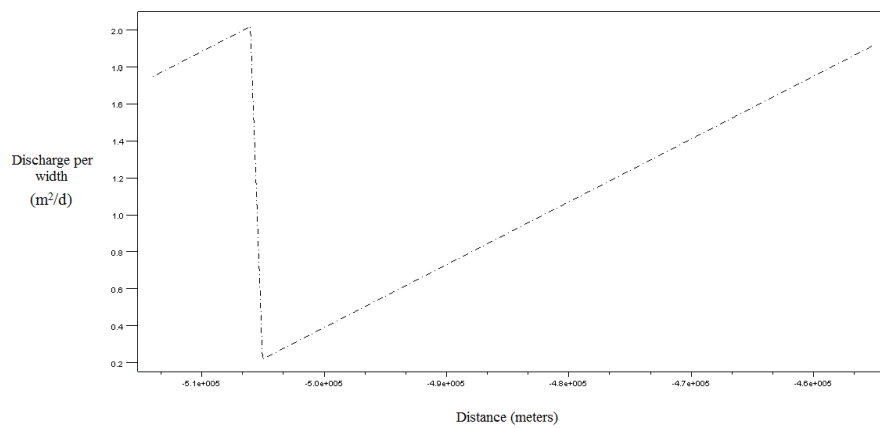


Figure 4.6: Discharge graph for the transect crossing Republican River.



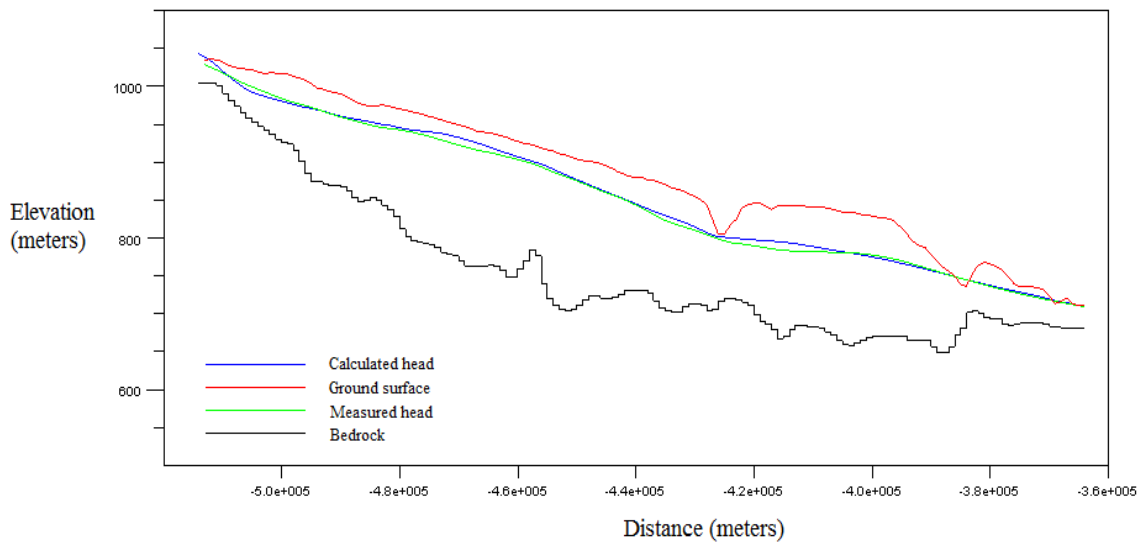


Figure 4.7: Model result in the transect crossing Cimarron River and Spring Creek.

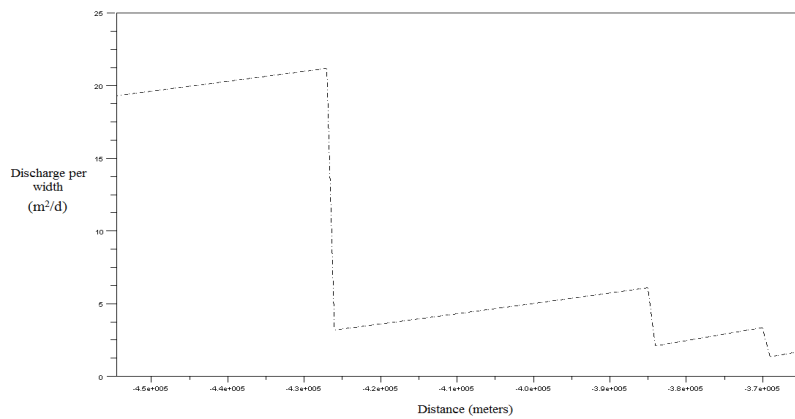
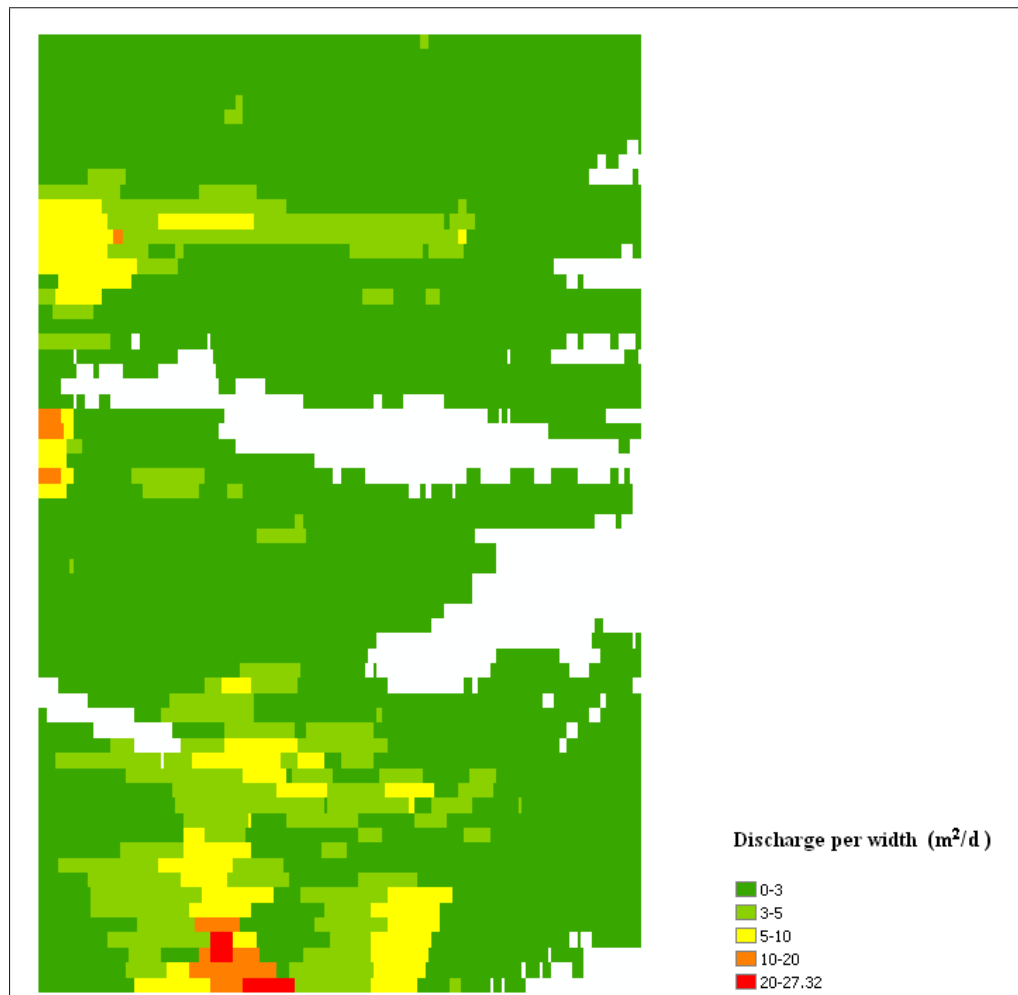


Figure 4.8: Discharge graph for the transect crossing Cimarron River and Spring Creek.

Figures 4.6 and 4.8 show groundwater discharge pattern in the aquifer as water moves from left to right. Abrupt change of discharge in the graphs show points where enough quantity of water was taken out to achieve mass balance, it can also be seen from the graphs how recharge is trying to replenish the lost water in the aquifer system. This approach was applied to all west-east transects and figure 4.9 shows overall variation in groundwater discharge across the entire Ogallala Aquifer as estimated by the model. Looking at difference in colors, points where water was taken out can also be identified from this figure. These points are clearly shown in figure 4.11. These are the points where groundwater discharges to surface water.



**Figure 4.9:** Variations in discharge per unit width for the entire study region.

After overlaying stream network on these water out-take points, it can be seen that most of these points fall along stream lines, but some of them fall in areas where there seem not to be any interaction between groundwater and the surface (Fig. 4.10); according to the stream network map. This might be explained in the following ways: it is possible that there were some minor defects in the input data, since the only input data that represents predevelopment conditions is the groundwater level data. Therefore, there might have been some changes in the land surface and its features; especially streams for this case. This might be used to identify regions that previously had springs and streams which no longer exist.

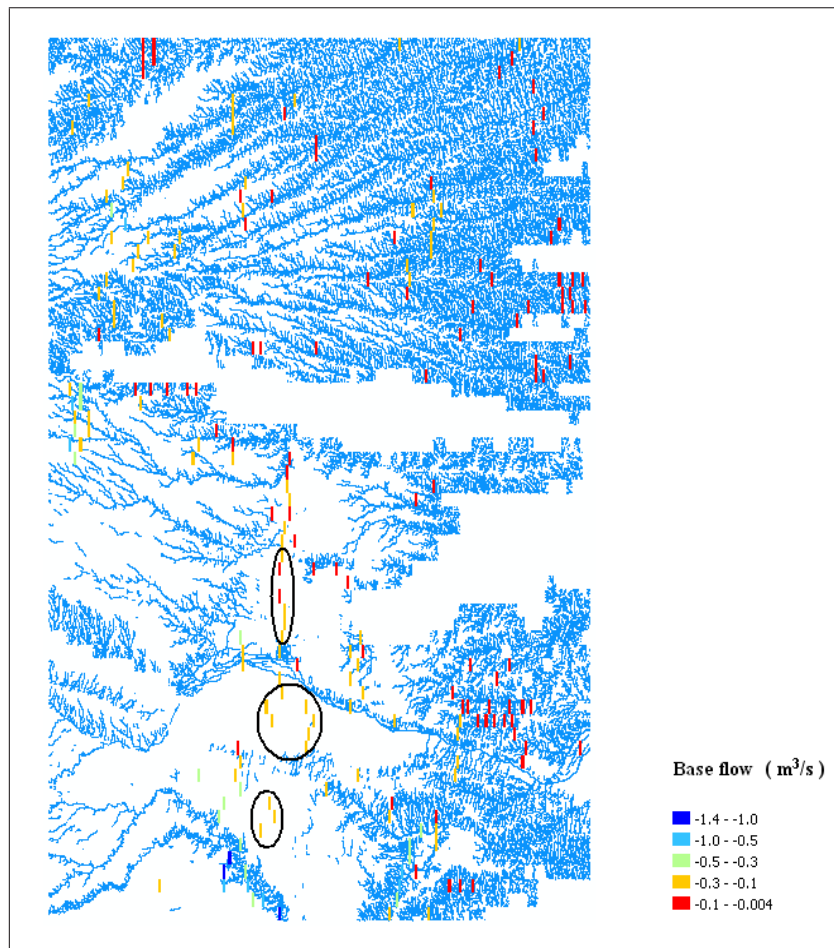


**Figure 4.10:** *Unaccounted-for Baseflow.*

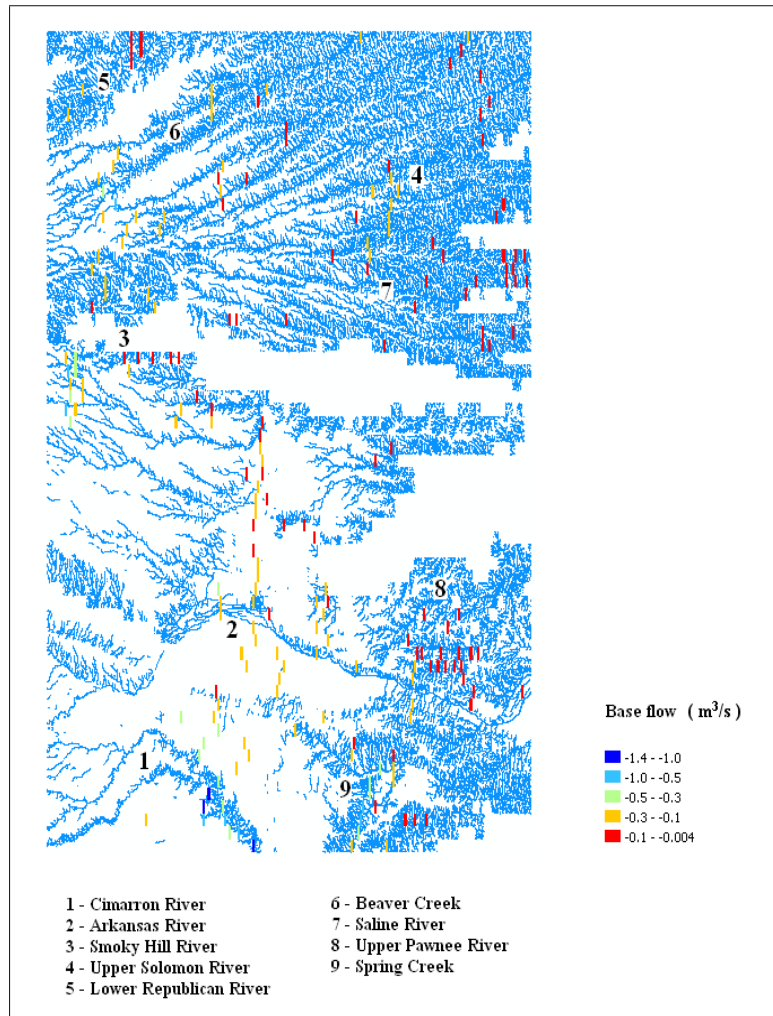


**Figure 4.11:** *Baseflow quantities at the groundwater-surface water interaction points.*

From figure 4.11, a closer look at the interaction between groundwater and surface water was done by looking at individual river basin in the Ogallala Aquifer region. Cumulative baseflow value was obtained for each of the major streams and compared to their historical streamflow data in the study region; this is shown and described in the following pages. This was done while trying to see the validity of the model results, and to understand the contribution of baseflow to the total streamflow during predevelopment conditions in these streams. Historical streamflow data for some of the streams could not be obtained.

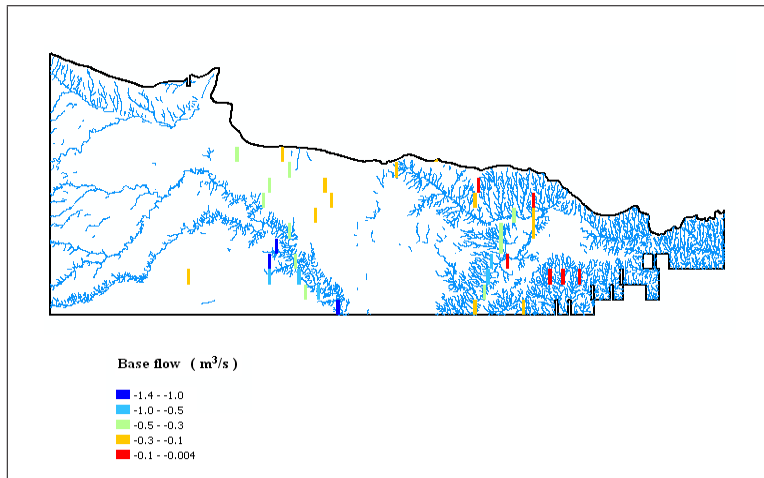


Figure 4.12: *Baseflow quantities in the Cimarron River Basin.*

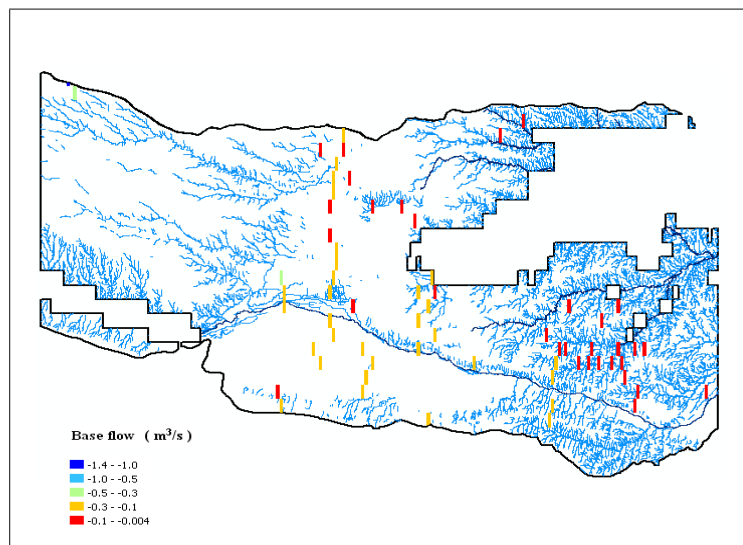
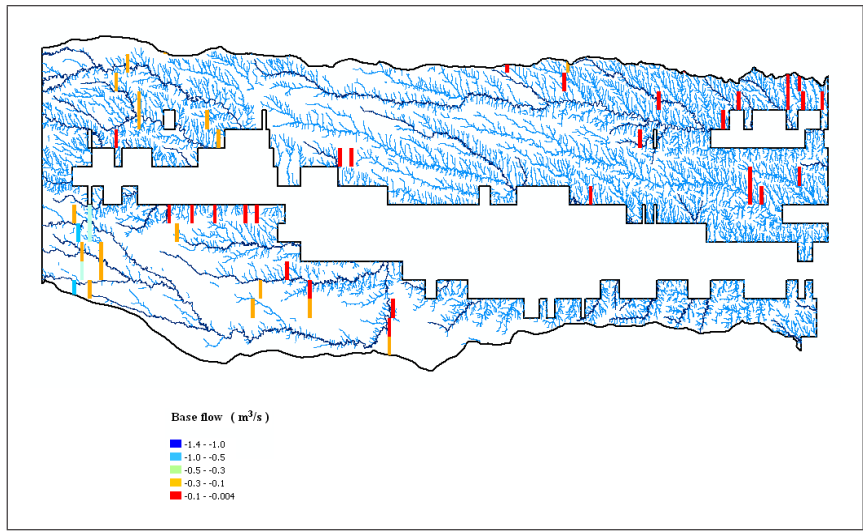
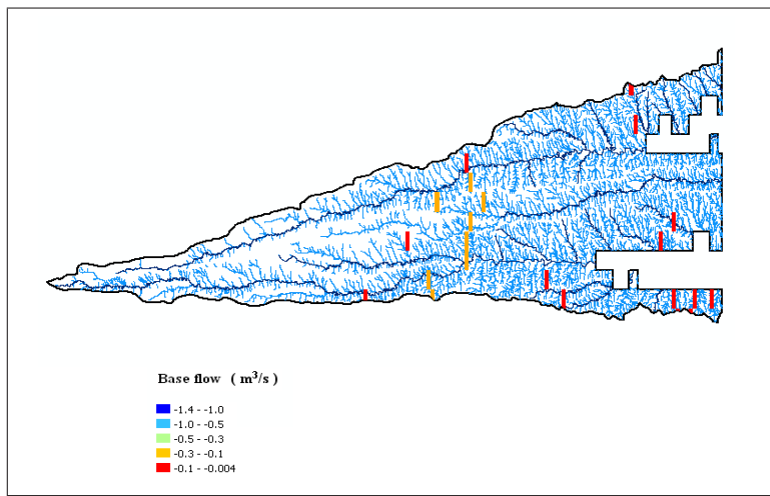


Figure 4.13: *Baseflow quantities in the Arkansas River Basin.*



**Figure 4.14:** *Baseflow quantities in the Smoky Hill River Basin.*



**Figure 4.15:** *Baseflow quantities in the Solomon River Basin.*

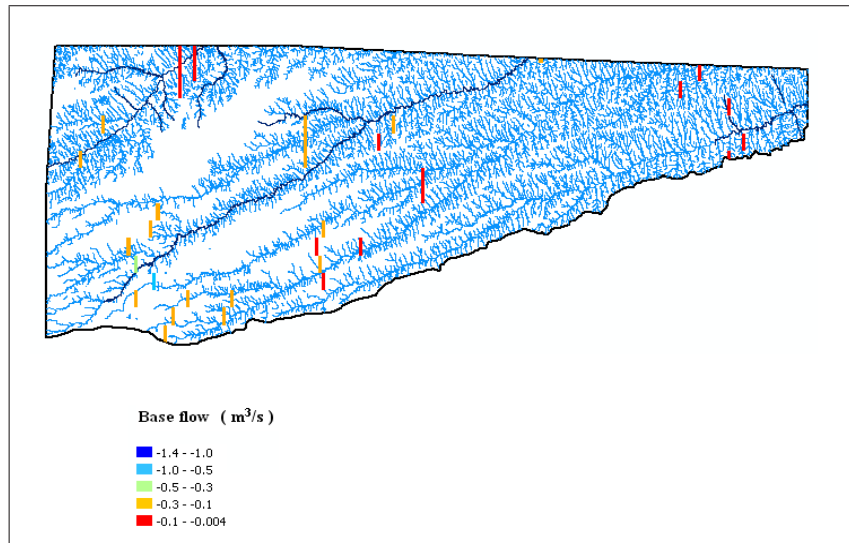


Figure 4.16: *Baseflow quantities in the Republican River Basin.*

The following streamflow data was obtained from the National Water Information System, United States Geological Survey (<http://www.gis.ksu.edu/ogallala>).

Year	Streamflow ( $m^3/s$ )
1966	4.100736
1967	2.80368
1968	2.177808
1969	2.217456
1970	1.85496
1971	1.767168
1972	2.832
1973	2.359056
1974	1.648224
1975	1.905936
1976	2.755536
1977	2.815008
1978	2.390208
1979	1.690704
1980	1.382016
1981	1.390512
1982	1.481136
1983	1.124304
1984	1.1328
1985	1.16112
1986	1.042176
1988	1.030848
1989	1.280064
1990	1.073328

Year	Streamflow ( $m^3/s$ )
1991	1.002528
1992	1.045008
1993	1.17528
1994	0.982704
1995	1.036512
1996	1.00536
1997	1.084656
1998	1.03368
1999	1.356528
2000	1.053504
2001	1.03368
2002	0.889248
2003	1.028016
2004	0.940224
2005	0.89208
2006	0.756144
2007	0.880752
2008	0.747648
2009	0.775968

**Table 4.1:** *Cimarron River streamflow data.*



Year	Streamflow ( $m^3/s$ )	Year	Streamflow ( $m^3/s$ )
1940	0.659856	1975	0.1829472
1941	3.05856	1976	0.1124304
1942	0.773136	1977	0.2245776
1943	0.1948416	1978	0.0506928
1944	0.43896	1979	0.1149792
1945	0.2211792	1980	0.1297056
1946	0.342672	1981	0.1101648
1947	2.104176	1982	0.0829776
1948	0.402144	1983	0.0688176
1949	1.580256	1984	0.0724992
1950	2.585616	1985	0.01214928
1951	8.2128	1986	0
1952	0.521088	1987	0.427632
1953	0.2370384	1988	0.021948
1954	0.1178112	1989	0.00280368
1955	1.517952	1990	0.1112976
1956	0.787296	1991	0.02829168
1957	4.519872	1992	0.0829776
1958	1.764336	1993	1.053504
1959	0.2359056	1994	0.0611712
1960	0.818448	1995	0.2749872
1961	0.716496	1996	0.76464
1962	1.039344	1997	0.171336
1963	0.0858096	1998	0.373824
1964	0.872256	1999	0.1427328
1965	0.2401536	2000	0.0342672
1966	0.506928	2001	0.1418832
1967	0.2483664	2002	0.01676544
1968	0.1294224	2003	0.00662688
1969	1.04784	2004	0.02104176
1970	0.1416	2005	0.01786992
1971	0.0974208	2006	0.0328512
1972	0.16284	2007	0.14868
1973	0.0917568	2008	0.0172752
1974	0.0589056	2009	0.0404976

**Table 4.2:** *Smoky Hill River streamflow data.*

Year	Streamflow ( $m^3/s$ )	Year	Streamflow ( $m^3/s$ )
1923	18.9036	1958	5.04096
1924	19.719216	1959	2.715888
1925	4.33296	1960	4.199856
1926	0.492768	1961	0.815616
1927	8.008896	1962	2.098512
1928	9.220992	1963	0.521088
1929	5.176896	1964	1.098816
1930	1.662384	1965	22.59936
1931	4.675632	1966	6.918576
1932	0.455952	1967	3.2568
1933	1.956912	1968	2.022048
1934	0.46728	1969	2.56296
1935	3.197328	1987	12.472128
1936	7.776672	1988	2.517648
1937	1.45848	1989	1.31688
1938	1.28856	1990	0.4248
1939	0.843936	1991	0.060888
1940	0.0521088	1992	0
1941	3.673104	1993	0.492768
1942	47.8608	1994	0.699504
1943	6.921408	1995	5.08344
1944	7.54728	1996	5.457264
1945	2.288256	1997	5.556384
1946	1.540608	1998	10.877712
1947	11.987856	1999	15.222
1948	2.956608	2000	5.256192
1949	8.742384	2001	3.231312
1950	5.454432	2002	0.600384
1951	12.327696	2003	0
1952	3.372912	2004	0
1953	1.158288	2005	0
1954	1.438656	2006	0
1955	2.02488	2007	0.00209568
1956	1.028016	2008	0.00167088
1957	2.37888	2009	0.00317184

**Table 4.3:** *Arkansas River streamflow data.*

<b>Year</b>	<b>Streamflow (<math>m^3/s</math>)</b>
1956	0.376656
1957	2.798016
1958	1.00536
1959	0.288864
1960	1.971072
1961	1.959744
1962	1.291392
1963	0.4956
1964	0.1455648
1965	0.591888
1966	0.826944
1982	0.0699504
1983	0.0178416
1984	0.0518256
1985	0.0589056
1986	0.0089208
1987	0.2274096
1988	0.02327904
1989	0.0416304
1990	0.00277536
1991	0
1992	0.0484272
1993	1.871952
1994	0.45312

<b>Year</b>	<b>Streamflow (<math>m^3/s</math>)</b>
1995	1.26024
1996	0.489936
1997	0.328512
1998	0.407808
1999	0.682512
2000	0.2741376
2001	0.314352
2002	0.1365024
2003	0.01619904
2004	0.0529584
2005	0.01212096
2006	0.00050976
2007	0.489936
2008	0.1379184
2009	0.365328

**Table 4.4:** *Saline River streamflow data.*

Year	Streamflow ( $m^3/s$ )	Year	Streamflow ( $m^3/s$ )
1946	1.135632	1978	0.917568
1947	3.987456	1979	0.458784
1948	1.832304	1980	0.385152
1949	2.302416	1981	0.300192
1950	4.777584	1982	0.427632
1951	13.79184	1983	0.2806512
1952	1.761504	1984	0.436128
1953	0.654192	1985	0.216648
1954	1.107312	1986	0.543744
1955	0.331344	1987	0.75048
1956	0.39648	1988	0.2271264
1957	4.859712	1989	0.362496
1958	2.602608	1990	0.2514816
1959	0.83544	1991	0.0450288
1960	2.88864	1992	0.2625264
1961	2.441184	1993	4.281984
1962	3.749568	1994	2.135328
1963	1.761504	1995	3.14352
1964	0.69384	1996	1.577424
1965	1.452816	1997	1.197936
1966	1.563264	1998	1.520784
1967	0.348336	1999	1.10448
1968	0.515424	2000	0.753312
1969	1.028016	2001	0.818448
1970	0.433296	2002	0.416304
1971	0.331344	2003	0.0909072
1972	0.291696	2004	0.0518256
1973	0.617376	2005	0.1619904
1974	0.80712	2006	0.0926064
1975	2.0532	2007	0.597552
1976	0.370992	2008	0.897744
1977	0.543744	2009	1.956912

**Table 4.5:** *Solomon River streamflow data.*

Year	Streamflow ( $m^3/s$ )
1947	1.226256
1948	0.419136
1949	0.90624
1950	0.62304
1951	3.010416
1952	0.597552
1953	0.0756144
1954	0.055224
1955	0.0048144
1956	0.1801152
1957	2.050368
1958	0.773136
1959	0.2741376
1960	1.863456
1961	0.501264
1962	1.248912
1963	0.433296
1964	0.348336
1965	1.532112
1966	0.875088
1967	0.1523616
1968	0.0872256
1969	0.1127136
1970	0.0733488
1971	0.0674016
1972	0.1588752
1973	0.1212096
1974	0.2540304
1975	0.286032
1976	0.02373216
1977	0.082128
1978	0.02469504

Year	Streamflow ( $m^3/s$ )
1979	0.02599776
1980	0.00478608
1981	0.1183776
1982	0.0960048
1983	0.2455344
1984	0.0305856
1985	0.01339536
1986	0.00048144
1987	0.01206432
1988	0.02673408
1989	0.2129664
1990	0.00546576
1991	0
1992	0.00903408
1993	0.2327904
1994	0.2101344
1995	0.1209264
1996	0.498432
1997	0.2769696
1998	0.1158288
1999	0.0761808
2000	0.01240416
2001	0.00521088
2002	0.00005664
2003	0.00178416
2004	0.002124
2005	0.0026904
2006	0
2007	0.01744512
2008	0.0470112
2009	0.00557904

**Table 4.6:** *Beaver Creek streamflow data.*

Year	Streamflow ( $m^3/s$ )	Year	Streamflow ( $m^3/s$ )
1938	2.390208	1974	0.7788
1939	0.93456	1975	1.169616
1940	0.945888	1976	0.334176
1941	2.730048	1977	0.654192
1942	2.928288	1978	0.31152
1943	1.248912	1979	0.659856
1944	2.030544	1980	0.824112
1945	1.549104	1981	1.095984
1946	2.744208	1982	0.625872
1947	2.486496	1983	0.696672
1948	2.092848	1984	0.875088
1949	2.543136	1985	0.557904
1950	1.455648	1986	0.543744
1951	3.423888	1987	0.535248
1952	1.299888	1988	0.385152
1953	0.2772528	1989	0.46728
1954	0.498432	1990	0.444624
1955	1.1328	1991	0.521088
1956	0.705168	1992	0.960048
1957	3.387072	1993	0.645696
1958	3.092544	1994	0.569232
1959	1.234752	1995	0.560736
1960	1.297056	1996	0.543744
1961	1.01952	1997	0.515424
1962	1.498128	1998	0.379488
1963	0.89208	1999	0.370992
1964	0.883584	2000	0.2288256
1965	1.702032	2001	0.1212096
1966	1.733184	2002	0.0617376
1967	1.070496	2003	0.0354
1968	0.625872	2004	0
1969	0.753312	2005	0
1970	0.994032	2006	0
1971	0.773136	2007	0.02636592
1972	1.008192	2008	0.00841104
1973	1.248912	2009	0.286032

**Table 4.7:** *Republican River streamflow data.*

Year	Streamflow ( $m^3/s$ )	Year	Streamflow ( $m^3/s$ )
1925	0.965712	1956	0.303024
1926	0.337008	1957	3.72408
1928	0.843936	1958	8.238288
1929	1.209264	1959	1.294224
1930	0.407808	1960	2.993424
1931	1.226256	1961	1.390512
1932	0.393648	1962	3.647616
1933	2.262768	1963	1.00536
1934	0.747648	1964	0.498432
1935	4.610496	1965	1.254576
1936	1.1328	1966	0.1673712
1937	0.586224	1967	2.155152
1938	1.608576	1968	0.458784
1939	0.985536	1969	0.974208
1940	2.574288	1970	1.081824
1941	0.957216	1971	1.01952
1942	0.965712	1972	1.28856
1943	1.362192	1973	3.29928
1944	3.661776	1974	1.022352
1945	0.48144	1975	0.43896
1946	0.809952	1976	0.464448
1947	4.902192	1977	0.521088
1948	4.58784	1978	0.5664
1949	4.14888	1979	3.078384
1950	8.940624	1980	0.985536
1951	15.559008	1981	1.209264
1952	1.580256	1982	1.121472
1953	1.602912	1983	0.31152
1954	0.308688	1984	0.1280064
1955	2.030544	1985	0.033984

**Table 4.8:** *Pawnee river streamflow data.*

Table 4.8 *cont'd*

<b>Year</b>	<b>Streamflow (<math>m^3/s</math>)</b>
1986	0.489936
1987	2.59128
1988	0.0702336
1989	0.713664
1990	0.713664
1991	0
1992	0.954384
1993	4.075248
1994	0.188328
1995	0.506928
1996	2.353392
1997	2.200464
1998	1.178112
1999	0.444624
2000	0.331344
2001	0.713664
2002	0.0968544
2003	0.2090016
2004	0.557904
2005	0.01835136
2006	0.2727216
2007	1.365024
2008	0.543744
2009	0.589056



Cumulative baseflow by stream produced by the model was compared with the mean annual streamflow in the predevelopment conditions. Streamflow events that occurred before 1950 were considered as predevelopment, and those that occurred during and after 1950 were considered as post-development. Approximate percentage of cumulative baseflow to the total streamflow in the predevelopment conditions is shown in table 4.9.

Stream	Mean annual streamflow ( $m^3/s$ )			Cumulative baseflow ( $m^3/s$ )	Approx. percentage of streamflow (%)
	Pre development	Post development	Percentage decrease		
Cimarron River	$\geq 4.10$	1.50	$\geq 63.40$	5.50	100.00
Arkansas River	6.80	3.50	48.50	0.97	14.30
Smoky Hill River	2.30	0.53	76.90	1.70	73.90
Upper Solomon River	2.31	1.32	42.80	0.95	41.10
Lower Republican River	2.05	0.81	60.50	0.38	18.50
Beaver Creek	0.85	0.30	64.70	0.50	58.80
Saline River	$\geq 0.40$	0.31	$\geq 22.50$	0.25	62.50
Upper Pawnee River	1.74	1.59	8.62	0.22	12.60
Spring Creek	-	-	-	2.16	-

**Table 4.9:** *Approximate percentage of baseflow to the total streamflow.*

The accuracy of the model was then looked at by comparing the actual (measured) predevelopment groundwater elevations (*Appendix C*) to the calculated (model) predevelopment groundwater elevations (Fig. 4.17). The model was found to be always within -16 to +12 meters between observed values and the model results, with an average value of 0.15m and a root mean square error of 1.98m (Fig. 4.18).

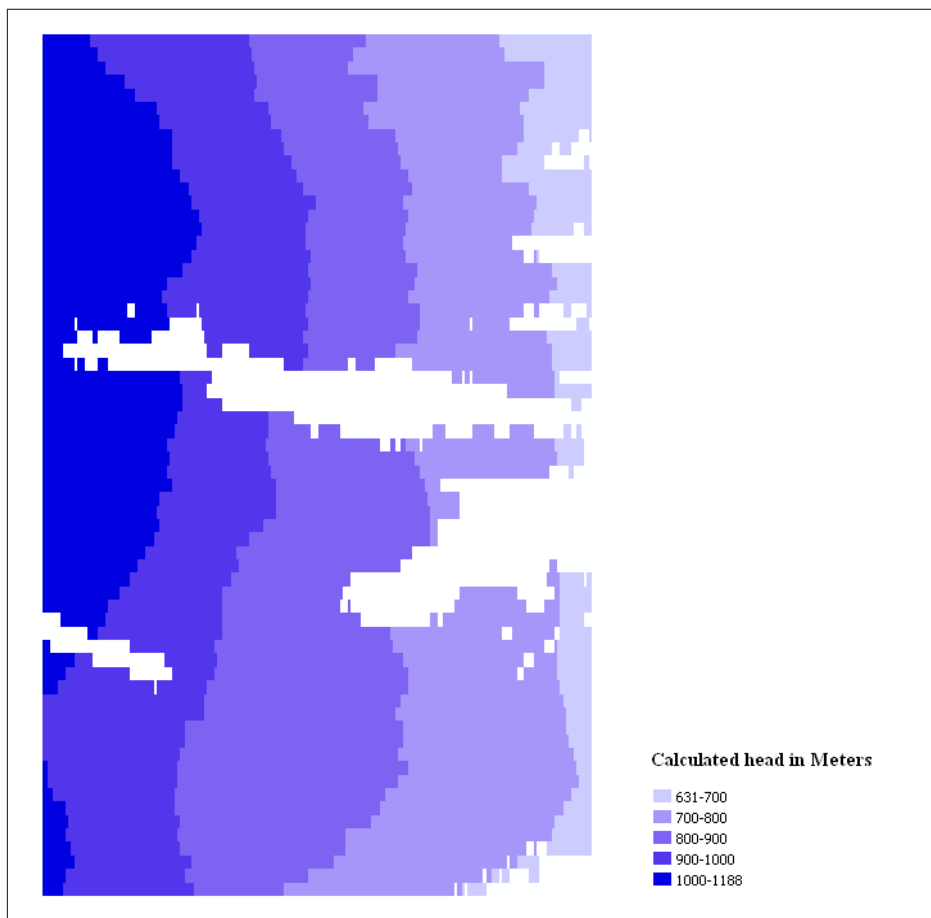


**Figure 4.17:** *Estimated groundwater elevations in the predevelopment conditions.*

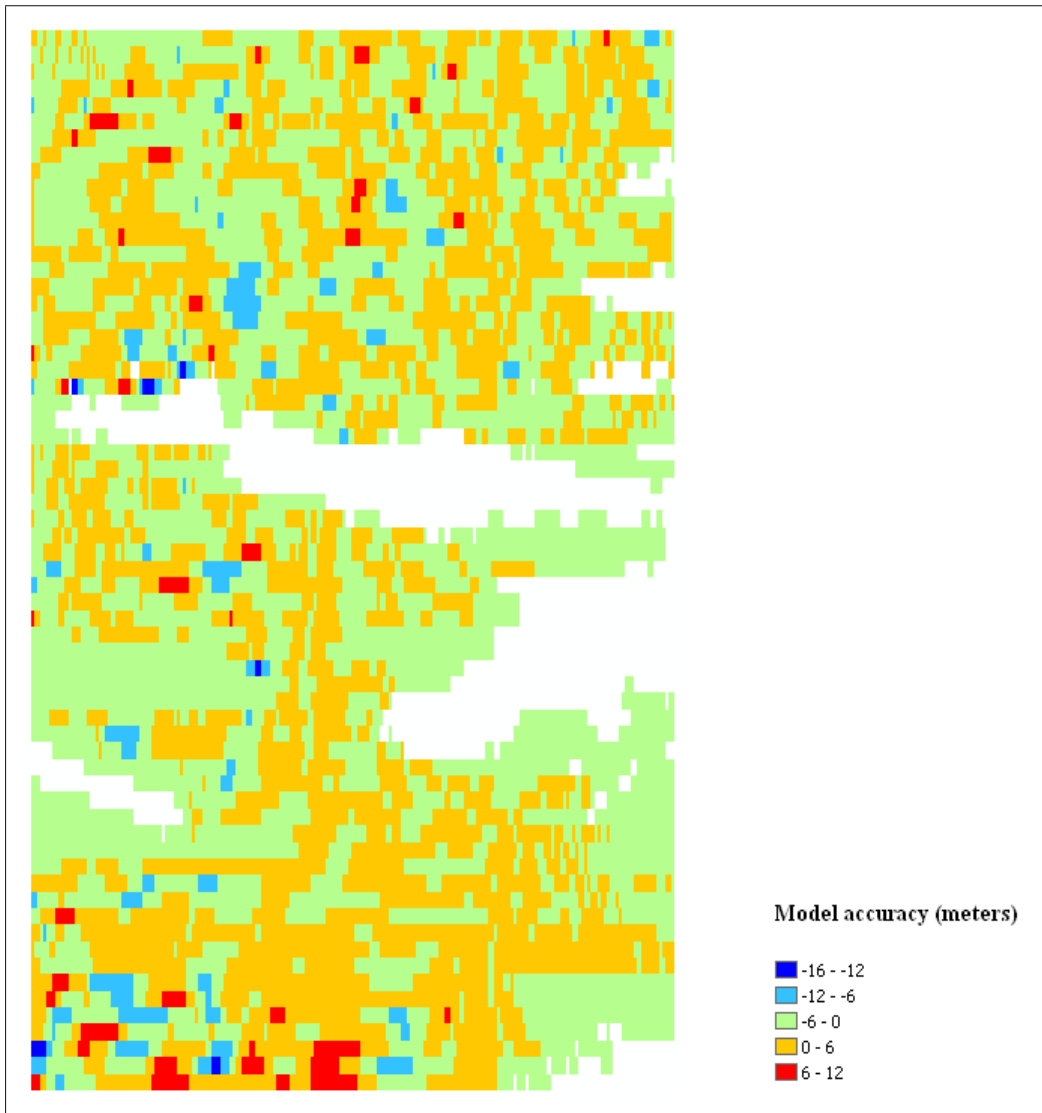


**Figure 4.18:** *Model accuracy; difference between approximated and actual values of head.*

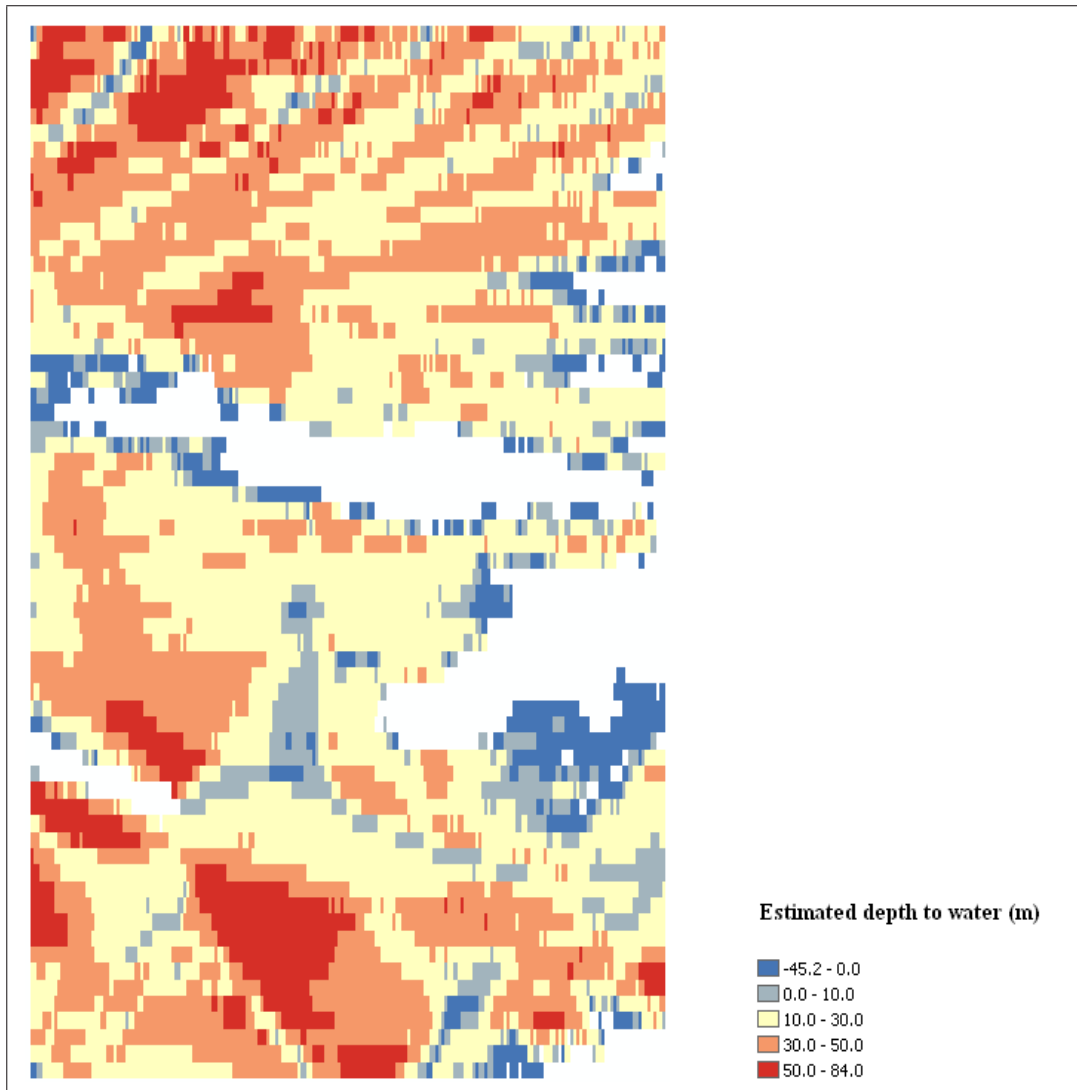


**Figure 4.19:** *Approximated depth to water in the predevelopment conditions.*

Quantification of groundwater discharge to streams in the predevelopment conditions was done while trying to understand long-term conservation of mass in the study region, these results can be used to try to understand the influence of climate change due to human activities to the behavior of groundwater flow in the study region in the long run. This can better be envisioned by the scenario of disappearing springs and stream which was discussed earlier in this study; this requires advancement of this work for further research.

Selection of the study area was based on the interest to study groundwater flow only for the Kansas portion of Ogallala Aquifer. Clipping of the Kansas portion of Ogallala Aquifer from the High Plains Aquifer was done for the following data: hydraulic conductivity, specific yield, bedrock elevation, and predevelopment water levels. Surface elevation and recharge data was obtained only for the State of Kansas. Therefore if this study is to be extended to study groundwater flow for the entire Ogallala Aquifer, then new data for recharge and surface elevation has to be obtained that cover the entire Ogallala Aquifer.

# Chapter 5

## Conclusions

The model was applied to simulate predevelopment groundwater conditions in the Ogallala Aquifer to understand long-term water balance in the study region. The conservation of mass was achieved by balancing groundwater input, output, and storage; this led to understanding the interactions of groundwater and surface water in the predevelopment conditions. The study resulted to identification of where natural discharge from groundwater to surface water occurred, and the quantity of these flows was obtained.

The Ogallala Aquifer is thick in the south western part of Kansas, this region had an average saturated thickness of 100m during predevelopment conditions. The model found that groundwater flowed at a discharge per width of approximately  $17 \text{ m}^2/\text{d}$  in this region. The aquifer thickness tends to gradually decrease from west to east and from south to north. The northern part had an average saturated thickness of 40m during predevelopment conditions; the model found that groundwater flowed at a discharge per width of approximately  $3 \text{ m}^2/\text{d}$  in this region. It was also found that groundwater leaves Ogallala Aquifer on the eastern side with discharge per width between  $0\text{-}3 \text{ m}^2/\text{d}$ .

The Discharge to streams necessary to satisfy long-term conservation of mass computed by the model showed that the cumulative baseflow by stream in the predevelopment conditions was found to vary from 0.22 to  $5.50 \text{ m}^3/\text{s}$  (Table 4.9), with the percentage of baseflow to the total streamflow in the predevelopment conditions varying from 12.6% to approximately 100%. Historical streamflow data for some of the streams e.g. Spring Creek could

not be obtained, this resulted to difficulty in understanding the contribution of baseflow to their total streamflow during predevelopment conditions.

Some groundwater-surface water interaction points identified by the model fall in areas where there seem not to be any interaction between groundwater and the surface; according to the stream network map. This might be explained in the following ways: it is possible that there were some minor defects in the input data, since the only input data that represents predevelopment conditions is the groundwater level data. Therefore, there might have been some changes in the land surface and its features; especially streams for this case. This might be used to identify springs and streams which no longer exist.

The model was found to be always within -16 to +12 meters between observed values and the model results, with an average value of 0.15m and a root mean square error of 1.98m. Results from this study can be used to advance this study to the next level by making a transient model that could be used as a predictive tool for groundwater response to water use in the study region.

# Bibliography

- [1] Bouwer, H. (1978), Groundwater Hydrology, *McGraw-Hill*, New York.
- [2] Brutsaert, W. (1994), The unit response of groundwater outflow from a hillslope, *Water Resour. Res.*, 30 (10), 2759- 2763.
- [3] Carslaw, H. S., and J. C. Jaeger (1959), Conduction of Heat in Solids, *Oxford Univ. Press*, New York.
- [4] Chapman, T. G. (2005), Recharge-induced groundwater flow over a plane sloping bed: Solutions for steady and transient flow using physical and numerical models, *Water Resour. Res.*, 41, W07027, doi:10.1029/2004WR003606.
- [5] Chapman, T.G., Modelling groundwater flow over sloping beds, *Water Resources Research*, 16 (6) , 1114-1118, 1980.
- [6] Chapman, T.G., and R.F. Dressler, Unsteady shallow groundwater flow over a curved impermeable boundary, *Water Resources Research*, 20 (10) , 1427-1434, 1984.
- [7] Chapman, T. G., and G. Ong (2006), A new equation for shallow groundwater flow over a curved impermeable boundary: Numerical solutions and laboratory tests, *Water Resour. Res.*, 42, W03427, doi:10.1029/2005WR004437.
- [8] Chauhan, H. S., G. O. Schwab, and M. Y. Hamdy (1968), Analytical and computer solutions of transient water tables for drainage of sloping land, *Water Resour. Res.*, 4 (3), 573- 579.
- [9] Childs, E. C. (1971), Drainage of groundwater resting on a sloping bed, *Water Resour. Res.*, 7 (5), 1256- 1263.



- [10] Daly, E., and A. Porporato (2004), A note on groundwater flow along a hillslope, *Water Resour. Res.*, 40, 1 - 5, W01601, doi:10.1029/2003WR002438.
- [11] Guitjens, J.C., and J.N. Luthin, Viscous model study of drain spacing on sloping land and comparison with mathematical solutions, *Water Resources Research*, 1 (4) , 523-530, 1965.
- [12] Gutentag, E.D., Heimes, F.J., Krothe, N.C., Luckey, R.R., and Weeks, J.B., 1984, Geohydrology of the High Plains aquifer in parts of Colorado, Kansas, Nebraska, New Mexico, Oklahoma, South Dakota, Texas, and Wyoming: *U.S. Geological Survey Professional Paper* 1400-B, 63 p.
- [13] Haitjema, H. M. (1995), Analytic Element Modeling of Groundwater Flow, *Elsevier*, New York.
- [14] Hansen, C.V. (1991), Estimates of freshwater storage and potential natural recharge for principal aquifers in Kansas. *Water-Resources Investigations Report* 87-4230, USGS, Reston, Virginia, 100 pp
- [15] Hantush, M. S. (1967), Growth and decay of groundwater mounds in response to uniform percolation, *Water Resour. Res.*, 3 (1), 227- 234.
- [16] Knight, J. H., M. Gilfedder, and G. R. Walker (2005), Impacts of irrigation and dry-land development on groundwater discharge to rivers - a unit response approach to cumulative impacts and analysis, *J. Hydrol.*, 303, 79- 91.
- [17] Koussis, A.D., A linear conceptual subsurface storm flow model, *Water Resources Research*, 28 (4) , 1047-1052, 1992.
- [18] Koussis, A.D., and L.-T. Lien, Linear theory of subsurface storm flow, *Water Resources Research*, 18 (6) , 1738-1740, 1982.

- [19] McDonald, M. G., and A.W. Harbaugh (1988), A Modular Three-Dimensional Ground-Water Flow Model, Book 6, Chap. A1, *U. S. Geological Survey Techniques of Water-Resources Investigations, U.S. Gov. Print. Off.*, Washington, D. C.
- [20] Montaigne, F. (2002), Water pressure, *Natl. Geogr.*, 9, 2 - 33.
- [21] Muskat, M. (1937), The Flow of Homogeneous Fluids Through Porous Media, *McGraw-Hill*, New York.
- [22] Pauwels, V. R. N., N. E. C. Verhoest, and F. P. De Troch (2002), A metahillslope model based on an analytical solution to a linearized Boussinesq equation for temporally variable recharge rates, *Water Resour. Res.*, 38 (12),1297, doi:10.1029/2001WR000714.
- [23] Polubarinova-Kochina, P. Y. (1962), Theory of Ground Water movement, *Princeton Univ. Press*, Princeton, N. J.
- [24] Schmid, P., and J. Luthin, The drainage of sloping lands, *Journal of Geophysical Research*, 69 (8) , 1525-1529, 1964.
- [25] Sloan, W.T., A physics-based function for modeling transient groundwater discharge at the watershed scale, *Water Resources Research*, 36 (1) , 225-241, 2000.
- [26] Stagnitti, F., L. Li, J.-Y. Parlange, W. Brutsaert, D. A. Lockington, T. S. Steenhuis, M. B. Parlange, D. A. Barry, and W. L. Hogarth (2004), Drying front in a sloping aquifer: Nonlinear effects, *Water Resour. Res.*, 40, W04601, doi:10.1029/2003WR002255.
- [27] Steward, D. R. (2007), Groundwater response to changing water-use practices in sloping aquifers, *Water Resour. Res.*, 43, W05408, doi: 10.1029/2005WR004837.
- [28] Strack, O. D. L. (1989), Groundwater Mechanics, *Prentice-Hall*, Upper Saddle River, N. J.
- [29] Strack, O. D. L. (2003), Theory and applications of the Analytic Element Method, *Rev. Geophys.*, 41 (2),1005, doi:10.1029/2002RG000111.

- [30] Towner, G.D., Drainage of groundwater resting on a sloping bed with uniform rainfall, *Water Resources Research*, 11 (1) , 144-147,1975.
- [31] Upadhyaya, A., and H. S. Chauhan (2001), Falling water tables in horizontal/ sloping aquifers, *J. Irrig. Drain. Eng.*, 127 (6), 378-384.
- [32] Verhoest, N. E. C., and P. A. Troch (2000), Some analytical solutions of the linearized Boussinesq equation with recharge for a sloping aquifer, *Water Resour. Res.*, 36 (3), 793-800.
- [33] Werner, P.W., Some problems in non-artesian ground-water flow, *Transactions of the American Geophysical Union*, 38 (4) , 511-518, 1957.
- [34] Wooding, R.A., and T.G. Chapman, Groundwater flow over a sloping impermeable layer. 1. Application of the Dupuit-Forchheimer assumption, *Journal of Geophysical Research*, 71, 2895-2902, 1966.
- [35] Youngs, E.G., Horizontal seepage through unconfined aquifers with hydraulic conductivity varying with depth, *Journal of Hydrology*, 3 , 283-296, 1965.

# Appendix A

## GIS Procedures

The following is the step by step description of the GIS procedures taken during data preparation. These routines and the corresponding python scripts were provided by Dr. Xiaoying Yang.

### A.1 Projection

Projection is the process of transforming three-dimensional space onto a two-dimensional map. This is done because maps are supposed to be flat, but the surfaces they represent are curved. All the digital data that was used for this modeling work was projected to one common coordinate system, *USA contiguous albers equal area conic (NAD 83) projection* system was used. Procedure for projection is the same for all the data.

#### Procedure:

1. Open ArcMap and add the data.
2. Open *arctoolbox* and then open *project tool*. This tool can easily be found by searching for the word *project* using the search tab in the arctoolbox window, or search for *project* raster when dealing with raster data.
3. Drag and drop the data to be projected into the *input dataset* field (it is better to

have all the data visible on the table of contents in ArcMap)

4. In the *output dataset* field, enter the path and name of the layer that will be generated. ArcMap usually fills this field automatically, but changes can be made.
5. Search for the type of projection system to be used in the *Output Coordinate System* field.
6. If the map is not in NAD 83 transformation, a prompt to define geographic transformation will appear, select *NAD 1927 to NAD 1983\_NADCON* transformation.
7. Click *ok*.

Since Kansas State is the area of interest, then only Kansas part of High Plains aquifer is needed. The area covering 50km linear distance around the outside of Kansas boundary was also included. To achieve this, *buffer* and *clip* tools were utilized.

## A.2 Buffering

Buffering is a process of defining a zone around a map feature measured in units of distance or time. For this study, the projected Kansas map included the area around the State with *50km* linear distance outside its boundary.

### Procedure:

1. Open ArcMap and add the projected Kansas map layer.
2. Open the arctoolbox, and then open *buffer* tool. This tool can easily be found by searching for the word *buffer* using the search tab in the arctoolbox window.
3. Drag and drop the Kansas map layer into the *input features* field.

4. In the *output feature class* field, enter the path and name of the layer that will be created. ArcMap usually fills this field automatically, but changes can be made.
5. In the *distance* field, select the *linear units*, and fill in *50*, with units of *km*.
6. Click *ok*.

### A.3 Clipping

Clipping is the process of obtaining a wanted region by elimination of parts of a data layer either inclusive or exclusive of given limits. Downloaded digital maps with data of High Plains aquifer, are supposed to be clipped to the buffered Kansas map, since Kansas is the area of interest for this study. Each layer is clipped to the Kansas map one at a time, and the same procedure is repeated to all of them. Hydraulic conductivity, specific yield, and predevelopment water level data are the ones which were clipped to Kansas map. Bedrock elevation, and recharge data was already within the Kansas boundary.

#### Procedure:

1. Open ArcMap and add the buffered Kansas map layer and all the layers to be clipped to Kansas map.
2. Open arctoolbox then open *clip tool*, search for the word *clip* in the arctoolbox window if the tool is not visible.
3. Drag and drop the layer to be clipped to Kansas map into the *input features* field.
4. Drag and drop the buffered Kansas map layer into the *clip features* field.
5. In the *output feature class* field enter the path and name of the layer that will be generated. ArcMap usually fills this field automatically, but changes can be made.
6. Click *ok*.

## A.4 Raster generation

Some of the original data appeared as lines e.g. bedrock elevation and predevelopment water level, some appeared as points e.g. wells, and other appeared as polygons e.g. hydraulic conductivity and specific yield. These data had to be transformed to raster format so as to have consistency in the data models.

### Procedure:

1. Drop all zero and below values in all the data. In ArcMap table of contents, right click on a layer that needs to be only with values greater than zero.
2. Click *open attribute table*, then click *options*, and then click *select by attributes*.
3. From the *select by attributes* dialog box, double click the field that needs to be with values greater than zero. The list of fields that are found in the attribute table of a layer, are the ones visible here. Complete the argument according to how the results need to be. Example, here the specific yield values needed are those above zero, the argument should be; e.g. "SY">0
4. Click *apply*, and close the *select by attributes* dialog box.
5. All values greater than zero will be highlighted in the attribute table and on the map. A layer with only the selected features needs to be created, which will be transformed to raster layer.
6. Right click on the layer with selected values, left click *selection*, and then click *create layer from selected features*.
7. A layer will be created and added, this is the one to be transformed to raster layer.

## **Polygons to raster**(feature to raster)

### **Procedure:**

1. Open the *spatial analyst tool*. To find this tool; click *view*, then go to *toolbars*, and then check *spatial analyst*. Otherwise, click *tools*, then click *customize* and check *spatial analyst*.
2. After the spatial analyst dialog box is opened, click the drop down arrow then go to *convert*, and then click *feature to raster*.
3. Drag and drop the layer to be transformed to raster into the *input features* field.
4. In the *field* section, select the field from the attribute table which was previously selected to remove values less or equal to zero.
5. In the *output cell size* field, specify the side dimension of the raster square.
6. In the *output raster* field, enter the path and name of the layer that will be created. ArcMap usually fills this field automatically, but changes can be made.

## **Lines to raster**(topo to raster)

### **Procedure:**

1. Open *arctoolbox* and then click the *search* tab at the bottom of arctoolbox window. Make sure that all the toolboxes have been added to arctoolbox window first.



2. Search for *topo to raster*.
3. When the search is complete, double click the *Topo to raster spatial analyst tool* to open it.
4. Drag and drop the layer to be transformed to raster into the *input feature data* field.
5. In the *output surface raster* field, enter the path and name of the layer that will be created. ArcMap usually fills this field automatically, but changes can be made.
6. In the *output cell size* field, specify the side dimension of the raster square, *100m* was specified for this work.
7. In the *drainage enforcement* field, select *NO\_ENFORCE*.
8. Click *ok*.

## A.5 Unit conversion

After creating raster layers, if there is a need to change units e.g. *feet to meter*. *Raster calculator* tool can be used to do unit conversion.

### Procedure:

1. Open the *spatial analyst* tool. To find this tool, click *view*, then go to *toolbars*, and then check *spatial analyst*. Otherwise, click *tools*, then click *customize* and check *spatial analyst*.
2. After the spatial analyst toolbar is opened, click the drop down arrow, and then select *raster calculator*.

3. A dialogue box will open which will allow conversion of units to be done, conversion is done by writing an argument similar to what is shown below;  
$$k\_m = [k\_ft] / 3.2808.$$
4. *k\_ft* is the name of data layer to be converted, and *k\_m* is the name of data layer that will be created after conversion process. Number 3.2808 is the conversion factor (feet to meter conversion). Double click on the existing layer to ensure that exact name of the layer to be converted appears on the square parenthesis.
5. After writing the conversion argument, click *evaluate* and a new layer will be created automatically.

## A.6 Permanent raster generation

This is the last step of data model transformation, the above generated raster layers can be called “temporary raster layers” and they need to be made permanent. i.e. If ArcMap is closed at this stage, all the raster layers that have been created will be lost.

### Procedure:

1. Right click a temporary raster layer, go to *data*, and then click *export data*.
2. A dialogue box will open, and some inputs needs to be specified.
3. In the *format* field choose *GRID*.
4. In the *location* field, enter the path to where the permanent raster layer that will be generated will be stored.
5. In the *name* field, put the name of the permanent raster layer that will be created.
6. Click *save*. If same name as that of temporary raster layer was used, a message will appear asking confirmation if same name is to be used.

## A.7 *Rename and point to raster shortcuts*

*Rename* and *point to raster* are text files that was created and used together with the *command line* tool in ArcMap to perform specific tasks. *Rename* shortcut was used to rename a batch of files (layer names) at once, there are occasions where this procedure is important. *Point to raster* shortcut was used to transform point shapefiles e.g. wells, to raster layers. **Note:** These shortcuts only work when data come from and is going to be stored in geodatabase.

### **Procedure:**

In order not to distort these text files (i.e. *rename* and *point to raster*), it is best advised to copy their contents to a new empty text file and make changes on the new file. Since there might be a lot of files to be renamed or point shapefiles that need to be converted to raster, it is better to utilize the *replace all* option found under *edit* tab to make changes to these text files. Changes that need to be made to these text files are; to specify the path from which the data come from, and to where the results are going to be stored. Therefore the paths locate where the geodatabase are, and their names. Remember to create a new empty geodatabase to store new files when using *point to raster* shortcut. For *rename* shortcut the paths are the same since only renaming is done, and not creating anything new. After making changes to the text files then copy the modified text to *command line* window in ArcMap, and then click *enter*. If red text appears then something is wrong, try to look for the problem and fix it. If green text appears then it is fine.

The following is a piece of contents of *rename* shortcut text file which was used with *command line* tool; it was used to rename all files which end with “\_1” to “\_Albers”. Note that the geodatabase is the same.

```
Rename_managementE:\RechargePaper\KSWaterUseTill2006.mdb\WIMASWells1960_1E:\RechargePaper\KSWaterUseTill2006.mdb\WIMASWells1960_Albers FeatureClass
```

```
Rename_managementE:\RechargePaper\KSWaterUseTill2006.mdb\WIMASWells1961_1E:\RechargePaper\KSWaterUseTill2006.mdb\WIMASWells1961_Albers FeatureClass
```

```
Rename_managementE:\RechargePaper\KSWaterUseTill2006.mdb\WIMASWells1962_1E:\RechargePaper\KSWaterUseTill2006.mdb\WIMASWells1962_Albers FeatureClass
```

The following is a piece of contents of *point to raster* shortcut text file which was used with *command line* tool; it was used to convert point shapefiles which end with “\_Albers”, to raster layers “WIMASWell19\*\*” and store them in a new geodatabase.

```
PointToRaster_conversionE:\RechargePaper\KSWaterUseTill2006.mdb\WIMASWells1959_Albers  
WU1959_TSValue E:\RechargePaper\KSWaterUseGridAlbersTill2006.mdb\WIMASWell1959 SUM NONE 100
```

```
PointToRaster_conversionE:\RechargePaper\KSWaterUseTill2006.mdb\WIMASWells1960_Albers  
WU1960_TSValue E:\RechargePaper\KSWaterUseGridAlbersTill2006.mdb\WIMASWell1960 SUM NONE 100
```

```
PointToRaster_conversionE:\RechargePaper\KSWaterUseTill2006.mdb\WIMASWells1961_Albers  
WU1961_TSValue E:\RechargePaper\KSWaterUseGridAlbersTill2006.mdb\WIMASWell1961 SUM NONE 100
```

## A.8 Development of geodatabase for WIMAS data

The water use data requested from WIMAS came in Microsoft office Access format. A database had to be developed from this Access data file that was going to be used for extraction of shapefiles from it to another geodatabase using python script. This process was done so as to develop ArcGIS compatible data.

### Procedure:

1. Open the WIMAS Access file and then open the table which contains the data. There is a need to query unique wells only from this table.

2. Open new query. This is done by clicking *query*, then clicking *design view*, and then click *ok*.
3. Drag and drop or just double click the different fields from the queried table to the new query/table to be developed. Examples of the fields that were used are; PDIV\_ID, COUNTY, TWP, TWP\_DIR, RNG, RNG\_DIR, SECT, LONGITUDE, LATITUDE, SOURCE, and PLSS. (PLSS was not created at this stage, write “G” as the Criteria for SOURCE).
4. Right click anywhere on an empty space, then click *Properties*. Set “*unique values*” to “*yes*”, and then close the box. Save the query and then run it.
5. Add the PLSS field. It should be defined as follows;  
 PLSS: [TWP] & [TWP\_DIR] &” ”& [RNG] & [RNG\_DIR] &” ”& [SECT]  
 After writing **PLSS:** in the column field space, click *Build* button, select by left clicking the query in question and it will be highlighted, its fields will show up to the right. Double click fields needed in the expression to complete it.
6. Click *ok*. ( remember to check/tick all the fields that needs to appear on the table)
7. Run the query again.
8. In the *design view*, click *query* and then click *make table query*. Enter the name of the table under current database, and then click *ok*.
9. Click the *Run* button. (a message will show up, click *ok*)
10. Open ArcCatalog and create a new personal geodatabase under a certain folder.
11. Right click the new empty geodatabase that has just been created, click *import* and then click *XML Workspace Document*. A XML window will open, choose “*schema only*” and specify the XML source to import by locating the ArcHydro XML. Click *next*, and then click *Finish*.

12. Click the refresh button in ArcCatalog, the new geodatabase should have some contents in it, although those contents are empty for now.
13. Open ArcMap, and then open a new empty map. Go to *tools* and click *add XY data*. Browse for the table that was created from Access query, fill *longitude* in the XField, and *latitude* in the YField. In the same dialog box, click *edit* and then click *Select*, then go to *geographic Coordinate System > North America > North America Datum 1927.prj*. Click *Add > Apply*, and then click *ok* twice.
14. A warning message will appear telling you that the generated table has no object ID, click *ok*. A layer will be automatically created with attribute table same as the Access table.
15. Project this layer to *USA contiguous albers equal area conic projection*, and change it from NAD 27 to NAD\_83\_NADCON. After projection, open the *attribute table* of this layer and *add a field* called PDIV txt. A warning message might show up, just close it.  
**Note:** Be sure to add and use current layer in ArcMap, do not confuse between the old unprojected layer and the projected one.
16. After entering the name of the new field as PDIV txt, change its type to *text*, and then click *ok*. This field needs to be made equal to PDIV\_ID field, with the difference that one is in number type and the other is in text type.
17. Right click the PDIV txt field head and then click *field calculator*. A warning message will show up, click *yes*, and the field calculator window will appear.
18. Double click PDIV\_ID from the window, which will make PDIV txt = [PDIV\_ID]. Click *ok* and close the attribute table.
19. Open *arctoolbox* and search for the word *extract*, and then select by double clicking “*Extract values to points*”.

20. In the *input point features* field, drag and drop the very recent layer of wells that was created and projected to Albers. In the *input raster* field, put in the surface elevation layer (DEM), remember that both layers should be in the same coordinate system.
21. In the *output point feature* field enter the path and name of the layer that will be generated. Without checking any of the boxes, click *ok* and then click *close*.
22. Open ArcCatalog and go to the new geodatabase that was created recently, expand it and right click *hydrogeology > properties > XY coordinate system*. Project it to Albers, NAD 83, since the schema was in UTM projection. Everything under hydrogeology will be projected to the same coordinate system.
23. Under *hydrogeology*, right click *well* then left click *load > load data > next*, open and add the shapefile of wells with elevation that was created in step 21, and then click *next*. Choose to *load all features into a subtype*, and *WIMAS point of diversion*, then click *next*.
24. Match *hydrocode* with *PDIV txt*, and *elevation* with *rasterVALU*, and then click *next*. Choose to *Load all of the source data* then click *next* and *finish*.
25. Go to ArcMap and add *well* and *hydroID table* layers both from the new geodatabase. From *editor* toolbar, click *editor > Start Editing > Select folder with hydroID table > ok > Start Editing*.
26. Open *hydroID table* by right clicking it and then click *open*. Write *others* in the first column of the first row, and put number *zero* in the second column of the first row. Close the box after writing, then click *editor > save edits*, and then click again *editor > stop editing*. Close the editor toolbar.
27. From *archydro* toolbar click *ApUtilities*, and then click *assign unique ID*. Highlight by left clicking *well* from the layers window that will appear, choose *yes* and *all features*

in the selection options, and then click *ok* twice. If the attribute table for the *well* layer is opened at this stage, *hydroID* column won't contain null values.

28. Open Microsoft office Access, click *file > get external data > import*, locate *well* in the database and click *ok*. Double click *well* and go to *design view*, change *hydrocode* to *number* data type and *field size* to *double*, then *save* and *close*.
29. While still in MS Access, open the access file with all the tables that are to be queried. In this case a table is to be developed from querying *water use table* and *well table*, therefore these tables must appear in one Access file.
30. Click *query > new query > design view* or just *query > create query in design view*. Add all the tables to query from and then close the box with the list of tables. Query the following fields from the *water use table*; WR\_ID, UMW\_CODE, PDIV\_ID, WUAPERS\_ID, WUACOR\_NUM, WUA\_YEAR, FO\_NUM, SOURCE, and AF\_USED. Write "G" as the criteria for SOURCE. Query *hydroID* field from *well table*. In case something else needs to be queried from a table that is already closed, right click anywhere in the empty space and click *show table*, and *add the table*.
31. After adding all the fields in the new query/table, click and drag *PDIV\_ID* from *water use table* window and drop it in *hydrocode* in the *well table* window. Then *run* the query and save it.
32. Create another query from the one developed in stage 31. It should be comprised of the following fields from the existing query (from step 31); HydroID, WUA\_YEAR, AF\_USED, and add two new fields, WUDate and TsType.
33. The two new fields should be defined as follows;  
**WUDate: CDate("12/31/" & Name of the existing query!WUA\_YEAR)**  
**TsType: 1**  
**Note:** A field can be conveniently defined by clicking the *build* button when the cursor



is in front of the field name e.g. WUDate:|

CDate is found in *functions > built in functions > conversion*, then double click *CDate* to add it in the formula. The existing query is found in *Queries* after opening the Expression Builder/ Build icon. Modify the rest of the expression manually, and then click *ok*.

Check/tick all columns that need to appear in the table query. Click the summation sign to add the row for *Total*, all fields should appear as *Group by* in the *Total* row except for AF\_USED, which should be *Sum*. *Run* the query.

34. Make table query from this query. After running the query return to design view, right click anywhere on an empty space and then click *properties*, and set *unique values* to *yes* and then close the box. Save the query. (A query can always be called back for modification after it is closed). After saving the query, *run* it.
35. While still in design view, click *query > make table query*. Put in the name of the table under current database, and then click *ok*.
36. *Run* again the query. A message will appear, click *yes*.
37. Data needs to be loaded to *Time Series* in the database. Open ArcCatalog and go to the personal geodatabase that needs to be filled with data, under it there is a *Time Series* file, right click it then click *load > load data > next*. Locate the table in Access that was created in step 35, select it then click *open > add > click next* twice.
38. Equate *feature ID* to *hydro ID*, *TSType ID* to *TsType*, *TSDatetime* to *WUDate*, and *TSTValue* to *Sum of AF\_USED*. Click *next* then *select to Load all of the Source data*, and then click *next* and *finish*.

This is how water use data from WIMAS was stored in a personal geodatabase. Data from this geodatabase has to be extracted to another geodatabase which will store shape files.

**Procedure:**

Python script was used for extracting the data. Right click the python file and click *edit with IDAE*, the file will open and changes have to be made to it. Before making changes to the script make sure that there is a new empty personal geodatabase which will store the shapefiles extracted from the existing geodatabase. (Open ArcCatagol, right click a folder to store a new geodatabase, click *new* and then click *create new personal geodatabase*).

Make changes to the *input* and *output* path in the python script, *input path* is the path from which the first geodatabase is at (one which the data is extracted from, the one containing *Timeseries* and *Hydrogeology/wells*), and the *output path* is the path to which the new empty geodatabase is at.

**Example:**

```
in_db="C:\\Phil_Recharge\\StateGroundwaterAug08.mdb."
```

```
out_db="C:\\Phil_Recharge\\KSWaterUseTill2006.mdb."
```

Save changes to the script (click *save*, not *save as*), then click *run* and then click *run module*.

The following is the Python script that was used to achieve this.

```

# this script creates the WIMAS layers with water use for each year for certain points of diversions

# 4/2/2009

# Input: Source Geodatabase, beginning year, ending year, WIMAS feature type ID, and Output
Geodatabase

#Output: WIMASWellsxxxx (wimas well layers for each year with two new fields WaterUse and Year ) and
WaterUsexxxx table in the output geodatabase

# Import system modules

import sys, string, os, arcgisscripting

gp = arcgisscripting.create()

# Check out any necessary licenses

gp.CheckOutExtension("spatial")
gp.CheckOutExtension("3D")

# Load required toolboxes...

gp.AddToolbox("C:/Program Files/ArcGIS/ArcToolbox/Toolboxes/Spatial Analyst Tools.tbx")
gp.AddToolbox("C:/Program Files/ArcGIS/ArcToolbox/Toolboxes/Data Management Tools.tbx")
gp.AddToolbox("C:/Program Files/ArcGIS/ArcToolbox/Toolboxes/3D Analyst Tools.tbx")

#get the path of the groundwater database

#in_db=gp.GetParameterAsText(0)

#in_db="D:\\KSGeoDatabase\\State\\StateGroundWaterAugo8.mdb"

in_db="C:\\Phil_Recharge\\StateGroundWaterAugo8.mdb"

gp.addmessage(in_db)

well = in_db + "\\Hydrogeology\\Well"

TimeSeries = in_db + "\\TimeSeries"

#get the beginning and ending years

#beg_year=gp.GetParameterAsText(1)

#end_year=gp.GetParameterAsText(2)

beg_year='1958'

end_year='2006'

```

```

if not(beg_year.isdigit())or not(end_year.isdigit())or(int(end_year)<int(beg_year))or(int(beg_year)<0):
#raise "YearError"
gp.AddMessage("YearError")
#get the feature type values for the WIMAS wells
#wimasftype=gp.GetParameterAsText(3)
wimasftype='1'
#get the time series type for water use data
#wutstype=gp.GetParameterAsText(4)
wutstype='2'
#get the output geodatabase
#out_db=gp.GetParameterAsText(5)
#out_db="D:\RechargePaper\KSWaterUseTill2006.mdb"
out_db="C:\Phil_Recharge\KSWaterUseTill2006.mdb"
i=0
try:
for i in range(int(beg_year),int(end_year)+1):
#initialize the value for the new field
welllayer=out_db+"\\\\"+"WIMASWells"+str(i)
welllayername="WIMASWells"+str(i)
gp.AddMessage(welllayer)
# make the feature layers for the WIMAS wells for certain year
gp.MakeFeatureLayer_management(well,welllayername,"[Ftype]="+wimasftype)
WU = out_db+"\\WU"+str(i) # physical name for the water use table
WUName="WU"+str(i) #only the table name for the water use table without the physical path
SelCriteria="[TSTypeID]="+wutstype+" AND [TSValue]>0 AND [TSDatetime] =#12/31/"+str(i)+"#"
print SelCriteria

```

```

gp.AddMessage(SelCriteria)

# Process: Select the records for a particular year
gp.TableSelect_Analysis(TimeSeries,WU,SelCriteria)

#add join
gp.AddJoin_management(welllayername, "HydroID", WU, "FeatureID", "KEEP_COMMON")
gp.AddMessage("join created!")

# create the feature class for wimas wells joined with water use data for a particular year
gp.FeatureClassToGeodatabase_conversion(welllayername, out_db)

#gp.RemoveJoin(welllayername,WUName)

#gp.AddMessage("Success 5")

finally:
gp.AddMessage("exit!")

```

## A.9 Batch Projection

This type of projection is used when there are a lot of shapefiles that need to be projected at once. Example, after extracting the WIMAS water use data from the first geodatabase, water use data from 1958 to 2006 will be stored in a new geodatabase with one shapefile for each year. Projecting each shapefile one by one is going to be tedious, and that is when batch projection was used.

### Procedure:

1. Open arctoolbox after opening ArcMap, search for the word *project* and then open by double clicking *batch project*.
2. Assuming all the layers to be projected have been added to the table of contents in ArcMap, highlight all the layers to be projected to the same coordinate system, then drag and drop them into the *input features* field.

3. In the *output workspace*, select a place e.g a geodatabase or a folder which will be used to store the results.
4. In the *output coordinate system*, choose the type of coordinate system to be used to project the data and then click *ok*.

## A.10 Spatial Interpolation-Inverse Distance Weighted

This method creates surfaces from measured points, based on the extent of similarity. For example, if you have an area with some number of wells with water level measurements and you want to develop a water level surface for the entire area, this method can be utilized. From the attribute table of the layer with water level records, take note of the name of the field which shows water levels (this is the level of water in the well from the mean sea level).

### Procedure:

1. Open ArcMap and add the layer with water level records.
2. Open the *spatial analyst toolbar*. Make sure it is activated in the extensions.
3. From the spatial analyst toolbar, click the drop down arrow and select *interpolate to raster*, and then select *inverse distance weighted* method.
4. In the *input points*, put the layer with water level data.
5. Fill in the field from the attribute table with the water levels in the *Z value field*.
6. In the *power* field, usually a default value of 2 is kept.
7. In the *search radius type*, select *variable*.
8. In the *number of points* field, enter the number of wells e.g. 8, that will be used for evaluation during interpolation process.

9. Select *nil* in the *max. distance* field.
10. In the *output cell size* field, specify the cell size of the raster surface to be generated, *100m* was specified for this work.
11. Fill in the *path* and *name* of the raster layer that will be created in the *output raster* field.
12. Without checking any box, click *ok*.

## A.11 Generation of rectangles using Python script

At this point all the shapefiles have been converted to raster format, with raster cells of 100m x 100m. These raster layers need to be converted back to shapefiles. The shapefiles should be made of rectangular mesh made of 1000m x 5000m rectangles. Each rectangle will have a mean value for all the 100m x 100m raster cells contained in it, these mean values are the ones which were used in the modeling work. Python script was used to create a toolbox that was used to generate these rectangles from the raster layers and obtain mean values. The results were exported from ArcMap to text files and then opened and saved as comma-delimited (csv) format in MS Excel. Scilab can now read data directly from this (.csv) file format, and this completes the process of data preparation.

### Procedure:

1. Open ArcMap, then open *arctoolbox*. In the *arctoolbox* window, right click the arc-toolbox icon.
2. Click *add toolbox* and search for the *GROWE* tool then add It. This tool was created by coding with Python, and it was used to generate rectangles that will aggregate raster cells and obtain mean values. Expand the tool to see its contents.

3. Right click *aggregate grid cells* and then click *properties*, go to *source* tab and locate the *aggregate cells python* file, then click *apply* and *ok*. This step is to ensure that the right python file is being used.
4. Double click *aggregate grid cells*.
5. In the *workspace* field, enter the path to the workspace where output will be stored. This can be a folder, make sure that the name of this folder does not contain spaces. As a general rule, avoid spaces during naming files when working with ArcGIS.
6. In the *GDB\_Name* field, enter the name for the new geodatabase that will be created. This geodatabase will be stored in the workspace specified above.
7. In the *PolysFC\_Name* field, enter the name for the specific attribute of the data e.g. k, Sy, etc. This will help to know which data is stored in the geodatabase.
8. In the *input grid* field, enter the raster layer to be processed.
9. In the *cell width* field, enter the width of the rectangle. 1000m was used for this work.
10. In the *cell height* field, enter the height of the rectangle. 5000m was used for this work.
11. Click *ok*. A message will appear to indicate successful execution or not.

The following is the Python script that was used to create GROWE toolbox, which was used to achieve this.



```

# -----
# MakeGridCells.py
# August 4, 2009
# Usage: MakeGridCells <Workspace> <GDB_Name> <FDS_Name> <Input_Grid> <PolysFC_Name>
# -----

#Import system modules.
import sys, string, os, arcgisscripting

#Create the Geoprocessor and set overwrite to true.
gp = arcgisscripting.create(9,3)
gp.OverwriteOutput = True

#Process script arguments and derive some variables.
Workspace = gp.GetParameterAsText(0)
GDB_Name = gp.GetParameterAsText(1)
if GDB_Name == '#':
    GDB_Name = "HPAquifer" # Provide a default value if unspecified.
GDB = GDB_Name + ".gdb"
FDS_Name = gp.GetParameterAsText(2)
if FDS_Name == '#':
    FDS_Name = "AggregateCells" # Provide a default value if unspecified.
FDS = GDB + "/" + FDS_Name
PolysFC_Name = gp.GetParameterAsText(3)
if PolysFC_Name == '#':
    PolysFC_Name = "Attribute" # Provide a default value if unspecified.
PolysFC = FDS + "/" + PolysFC_Name
Input_Grid = gp.GetParameterAsText(4)
Cell_Width = gp.GetParameterAsText(5)
Cell_Height = gp.GetParameterAsText(6)

#Set the Workspace.

```

```

gp.Workspace = Workspace

#Determine spatial reference of Input_Grid for feature data set.

desc = gp.Describe(Input_Grid)
SpRef = desc.SpatialReference

#Verify that the Input_Grid is in projected space.

if SpRef.Type != "Projected":
    gp.AddMessage("Input raster data is not a projected data set.")
    sys.exit()

#Create the Geodatabase and empty Feature Data Set.

gp.AddMessage("Creating Geodatabase " + GDB_Name + " with Feature Data Set " + FDS_Name + "...")
gp.CreateFileGDB_management(Workspace, GDB_Name)
gp.CreateFeatureDataset_management(GDB, FDS_Name, SpRef)

#Specify names for feature classes of Fishnet Lines and Labels.

FishnetFC = FDS + "/Fishnet"
LabelsFC = FDS + "/Fishnet_label"

#Describe Input_Grid and derive extents.

desc = gp.Describe(Input_Grid)

Extent = desc.Extent

OriginPt = str(Extent.XMin) + " " + str(Extent.YMin)
AxisPt = str(Extent.XMin) + " " + str(Extent.YMin + 10)

#Calculate rows and columns needed for fishnet.

Rows = int(math.ceil((Extent.YMax-Extent.YMin)/int(Cell_Height)))
Cols = int(math.ceil((Extent.XMax-Extent.XMin)/int(Cell_Width)))

#Create fishnet lines and labels.

gp.AddMessage("Creating Fishnet with " + str(Rows) + " rows and " + str(Cols) + " columns at Origin Point: " + str(OriginPt) + "...")

gp.CreateFishnet_management(FishnetFC, OriginPt, AxisPt, Cell_Width, Cell_Height, Rows, Cols, "#", "labels", Input_Grid)

#Make feature layers of the Fishnet and Labels feature classes.

```

```

FishnetLyr = "FishnetLayer"
LabelsLyr = "LabelsLayer"

gp.MakeFeatureLayer_management(FishnetFC, FishnetLyr)
gp.MakeFeatureLayer_management(LabelsFC, LabelsLyr)

#Add X,Y coordinates to labels.
gp.AddMessage("Getting coordinates for cells...")
gp.AddXY_management(LabelsLyr)

#Create Polygons feature class from fishnet lines and labels.
gp.AddMessage("Creating Polygons Feature Class...")
gp.FeatureToPolygon_management(FishnetLyr, PolysFC, "#", "Attributes", LabelsLyr)

#Add ZONE_ID number and set it equal to ObjectID.
gp.AddMessage("Assigning Zone IDs...")
gp.AddField_management(PolysFC, "ZONE_ID", "long")
gp.CalculateField_management(PolysFC, "ZONE_ID", "[OBJECTID]")

#Calculate zonal statistics as a table.
gp.AddMessage("Calculating zonal statistics...")
Stat_Table = GDB + "/ZonalStats"
gp.ZonalStatisticsAsTable_sa(PolysFC, "ZONE_ID", Input_Grid, Stat_Table, "DATA")

#Join ZonalStats table to Polys FC.
gp.JoinField_management(PolysFC, "ZONE_ID", Stat_Table, "VALUE")

# Delete variables, releasing memory.
del gp, Workspace, GDB_Name, GDB, FDS_Name, FDS, PolysFC_Name, PolysFC, Input_Grid, Cell_Width,
Cell_Height

del desc, SpRef, FishnetFC, LabelsFC, Extent, OriginPt, AxisPt, Rows, Cols, FishnetLyr, LabelsLyr, Stat_Table

```

## Appendix B

### Computer program and Data input file



```

54
55 for i=1:max(size(data_xid))
56 printf("i %d\n",i);
57 if ~exists("slope") then
58     slopei.xid=data_xid(i);
59     slopei.yid=data_yid(i);
60     slopei.X =data_X (i);
61     slopei.Y =data_Y (i);
62     slopei.K=data_K(i);
63     slopei.Sy =data_Sy (i);
64     slopei.BDELV =data_BDELV (i);
65     slopei.PWL =data_PWL (i);
66     slopei.R =data_R(i);
67     slopei.SRELV =data_SRELV (i);
68     slopei.WU=data_WU(i,:);
69     slope=list(slopei);
70 else
71     found=%F;
72     for j=1:size(slope)
73         if slope(j).yid==data_yid(i) then
74             found=%T;
75             slope(j).xid=[slope(j).xid;data_xid(i)];
76             slope(j).yid=[slope(j).yid;data_yid(i)];
77             slope(j).X =[slope(j).X; data_X(i)];
78             slope(j).Y=[slope(j).Y;data_Y(i)];
79             slope(j).K=[slope(j).K;data_K(i)];
80             slope(j).Sy =[slope(j).Sy; data_Sy(i)];
81             slope(j).BDELV=[slope(j).BDELV;data_BDELV(i)];
82             slope(j).PWL =[slope(j).PWL; data_PWL(i)];
83             slope(j).R =[slope(j).R; data_R(i)];
84             slope(j).SRELV=[slope(j).SRELV;data_SRELV(i)];
85             slope(j).WU =[slope(j).WU; data_WU(i,:)];
86         end
87     end
88     if ~found then
89         slopei.xid =data_xid(i);
90         slopei.yid =data_yid(i);
91         slopei.X =data_X (i);
92         slopei.Y =data_Y (i);
93         slopei.K =data_K(i);
94         slopei.Sy =data_Sy (i);
95         slopei.BDELV =data_BDELV (i);
96         slopei.PWL =data_PWL (i);
97         slopei.R =data_R (i);
98         slopei.SRELV =data_SRELV (i);
99         slopei.WU =data_WU(i,:);
100         slope($+1)=slopei;
101     end
102 end
103 end

```

```

104
105 // Specifying starting head and discharge per width
106 // in the jth transect.
107
108     j=11;
109
110     phi2=slope(j).PWL($);
111     Q0=1;
112
113 i=max(size(slope(j).X));
114 for i=[max(size(slope(j).X):-1:2]
115
116
117     L=slope(j).X(i)-slope(j).X(i-1);
118     x    =[0:L:L];
119     k    =slope(j).K(i);
120     Sy   =slope(j).Sy(i);
121     R    =slope(j).R(i);
122     Land =slope(j).SRELV(i);
123     B    =slope(j).BDELV(i);
124     PWL  =slope(j).PWL(i);
125     X    =slope(j).X(i);
126
127 l=max(size(x))-1;
128 for l=[max(size(x))-1:-1:1]
129
130     // Calculating Potential, head, and discharge per width
131
132     Phi2=0.5*k*(phi2-B).^2;
133     Phi=-R/2*(x(l)-x(l+1)).^2-Q0*(x(l)-x(l+1))+Phi2;
134     phi2=B+sqrt(2*Phi/k);
135     Q0=Q0+R*(x(l)-x(l+1));
136
137
138 // Printing results in matrix form
139
140 if l==max(size(x))-1 then
141
142     h=phi2;
143     b=B;
144     Q=Q0;
145     p=PWL;
146     s=Land;
147     ex=X;
148 else
149     h=[h,phi2];
150     b=[b,B];
151     Q=[Q,Q0];
152     p=[p,PWL];
153     s=[s,Land];
154     ex=[ex,X];
155 end
156

```

```

157 l=l-1;
158 end
159
160 if i==max(size(slope(j).X)) then
161     H=h;
162     Bb=b;
163     Qx=Q;
164     pw=p;
165     se=s;
166     exx=ex;
167 else
168     H=[H,h];
169     Bb=[Bb,b];
170     Qx=[Qx,Q];
171     pw=[pw,p];
172     se=[se,s];
173     exx=[exx,ex];
174 end
175
176 i=i-1;
177 end
178
179 // Reading results and plotting
180
181 disch=[1,Qx];
182 Head=[slope(j).PWL($),H];
183 Discharge=disch($:-1:1);
184 head=Head($:-1:1);
185 base=[Bb($:-1:1),slope(j).BDELV($)];
186 pwl=pw($:-1:1);
187 sel=se($:-1:1);
188 xcord=exx($:-1:1);
189
190 Xcord=[slope(j).X(1):1000:slope(j).X($)];
191
192 plot(Xcord,head);
193 plot(Xcord,Discharge);
194 plot2d2(Xcord,base);
195 plot(xcord,pwl,'g');
196 plot(xcord,sel,'r');
197
198
199
200

```



## B.2 Sample data input file

Microsoft Excel - sloping\_base\_data.csv

File Edit View Insert Format Tools Data Window Help

Arial 10 B I U \$ %

	A	B	C	D	E	F	G	H	I	J	K	L	M	N	O	P
1	xid	yid	X	Y	K	Sy	BDELV	PWL	R	SRELV	WU58	WU59	WU60	WU61	WU62	WU63
2	1	1	-514044	-24558.5	7.619999	0.1	1004.63	1031.075	0.000036	1037.875	0	0	0	0	0	0
3	2	1	-513044	-24558.5	7.619999	0.1	1003.859	1028.491	0.000037	1034.647	0	0	0	0	0	0
4	3	1	-512044	-24558.5	7.619999	0.082599	1003.641	1025.432	0.000037	1036.245	0	0	0	0	0	0
5	4	1	-511044	-24558.5	7.619999	0.0625	1004.486	1021.936	0.000037	1035.007	0	0	0	0	0	0
6	5	1	-510044	-24558.5	7.619999	0.0608	1001.199	1018.213	0.000038	1032.591	0	0	0	0	0	0
7	6	1	-509044	-24558.5	7.619999	0.0705	990.923	1014.215	0.000038	1028.251	0	0	0	0	0	0
8	7	1	-508044	-24558.5	7.619999	0.0642	981.4987	1009.898	0.000038	1025.122	0	0	0	0	0	0
9	8	1	-507044	-24558.5	7.619999	0.1018	973.6197	1006	0.00004	1024.052	0	0	0	0	0	0
10	9	1	-506044	-24558.5	7.619999	0.12	965.452	1002.7	0.00004	1022.694	0	0	0	0	0	0
11	10	1	-505044	-24558.5	10.63752	0.1388	958.2557	999.5061	0.00004	1021.895	0	0	0	0	0	0
12	11	1	-504044	-24558.5	15.24	0.1498	952.12	996.3635	0.000041	1019.1	0	0	0	0	0	0
13	12	1	-503044	-24558.5	15.24	0.15	946.869	993.189	0.000042	1017.359	0	0	0	0	0	0
14	13	1	-502044	-24558.5	15.24	0.157499	942.2645	990.0635	0.000042	1017.777	0	0	0	0	0	0
15	14	1	-501044	-24558.5	15.24	0.182	936.6522	987.0705	0.000043	1017.661	0	0	0	0	0	0
16	15	1	-500044	-24558.5	15.24	0.1903	930.4638	984.1898	0.000043	1017.66	0	0	0	0	0	0
17	16	1	-499044	-24558.5	15.24	0.197099	926.3865	981.4373	0.000043	1016.622	0	0	0	0	0	0
18	17	1	-498044	-24558.5	15.24	0.198899	923.7447	978.9391	0.000044	1013.084	0	0	0	0	0	0
19	18	1	-497044	-24558.5	15.24	0.1912	915.7097	976.7009	0.000045	1011.04	0	0	0	0	0	0
20	19	1	-496044	-24558.5	15.24	0.1855	901.2744	974.7483	0.000045	1008.239	0	0	0	0	0	0
21	20	1	-495044	-24558.5	15.14856	0.180299	884.856	972.5521	0.000046	1004.17	0	0	0	0	0	0
22	21	1	-494044	-24558.5	13.15212	0.1736	875.2062	969.9658	0.000047	998.2026	0	0	0	0	0	0
23	22	1	-493044	-24558.5	10.54608	0.1657	873.9681	967.2874	0.000047	996.2072	0	0	0	0	0	0
24	23	1	-492044	-24558.5	9.357359	0.148699	871.2076	964.6539	0.000048	993.6992	0	0	0	0	0	0
25	24	1	-491044	-24558.5	9.906	0.1378	869.0125	962.1371	0.000048	991.8932	0	0	0	0	0	0
26	25	1	-490044	-24558.5	11.38428	0.1318	868.6807	959.7647	0.000048	990.0266	0	0	0	0	0	0
27	26	1	-489044	-24558.5	13.76172	0.1277	868.3638	957.5087	0.000049	986.74	0	0	0	0	0	0
28	27	1	-488044	-24558.5	15.24	0.1253	862.7189	955.3156	0.00005	982.1481	0	0	0	0	0	0
29	28	1	-487044	-24558.5	15.24	0.1238	852.5225	953.1699	0.00005	977.8038	0	0	0	0	0	0
30	29	1	-486044	-24558.5	15.24	0.1227	847.4129	951.053	0.000051	975.7881	0	0	0	0	0	0
31	30	1	-485044	-24558.5	15.24	0.1217	850.3224	948.9939	0.000051	973.4748	0	0	0	0	0	0
32	31	1	-484044	-24558.5	15.24	0.1243	853.7925	947.1465	0.000051	973.6158	0	0	0	0	0	0
33	32	1	-483044	-24558.5	15.33144	0.1342	850.2084	945.702	0.000053	975.8458	0	0	0	0	0	0
34	33	1	-482044	-24558.5	27.82824	0.1409	843.4666	944.6913	0.000053	974.0397	0	0	0	0	0	0
35	34	1	-481044	-24558.5	30.48	0.15	837.2145	943.7698	0.000053	972.0603	0	0	0	0	0	0
36	35	1	-480044	-24558.5	30.48	0.15	828.5123	942.6761	0.000054	970.5212	0	0	0.250796	0.281216	0	0.492
37	36	1	-479044	-24558.5	36.08832	0.154899	812.2547	941.3626	0.000054	968.6355	0	0	0	0	0	0
38	37	1	-478044	-24558.5	58.88736	0.1661	801.1164	939.8245	0.000054	966.6793	0	0	0	0	0	0
39	38	1	-477044	-24558.5	60.96	0.1771	796.2935	938.0587	0.000056	964.8262	0	0	0	0	0	0
40	39	1	-476044	-24558.5	60.96	0.2018	794.0065	936.0869	0.000056	963.2359	0	0	0	0	0	0
41	40	1	-475044	-24558.5	60.96	0.232899	792.2605	933.9585	0.000056	960.3137	0	0	0	0	0	0
42	41	1	-474044	-24558.5	60.96	0.25	790.316	931.7065	0.000058	958.6691	0	0	0	0	0	0

# Appendix C

## Input data

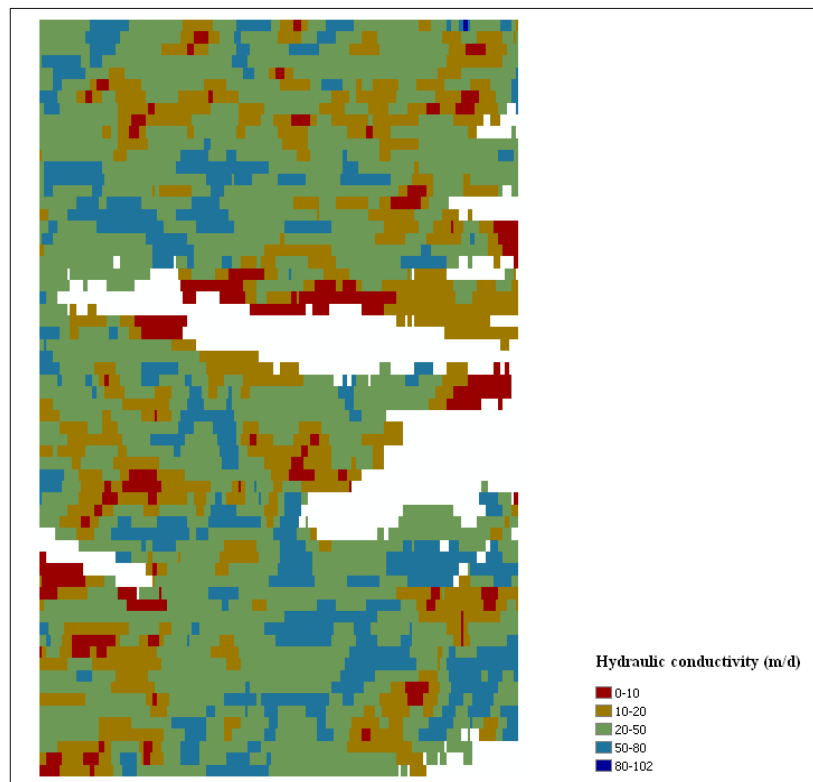
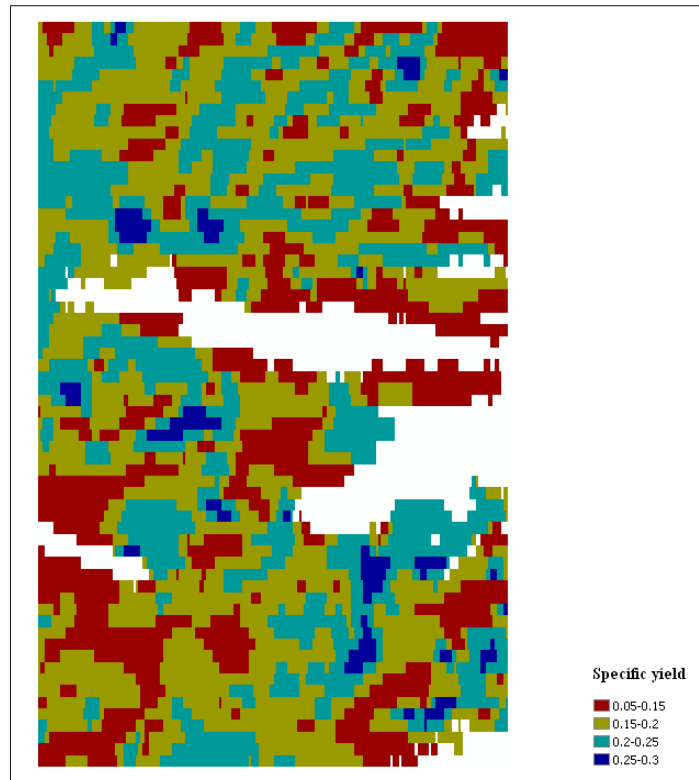


Figure C.1: *Hydraulic conductivity*

This data set consists of digital hydraulic conductivity rectangles for the portion of Ogallala Aquifer used in this study. It is a modified version of the digital data set that consisted of hydraulic conductivity contours and polygons for the High Plains aquifer in the central United States. The original digital data set was created by digitizing the hydraulic conductivity contours from a 1:1,000,000 base map created by the U.S. Geological Survey High Plains RASA project (Gutentag, E.D., Heimes, F.J., Krothe, N.C., Luckey, R.R., and Weeks, J.B., 1984, Geohydrology of the High Plains aquifer in parts of Colorado, Kansas, Nebraska, New Mexico, Oklahoma, South Dakota, Texas, and Wyoming: U.S. Geological Survey Professional Paper 1400-B, 63 p.) The original data was not supposed to be used at scales larger than 1:1,000,000.

Online linkage: <http://water.usgs.gov/lookup/getspatial?ofr98-548>



**Figure C.2:** *Specific yield*

This data set consists of digital specific yield rectangles for the portion of Ogallala Aquifer used in this study. It is a modified version of the digital data set that consisted of specific yield percentage contours and polygons for the High Plains aquifer in the central United States. The original digital data set was created by digitizing the specific yield percentage contours from a 1:1,000,000 base map created by the U.S. Geological Survey High Plains RASA project (Gutentag, E.D., Heimes, F.J., Krothe, N.C., Luckey, R.R., and Weeks, J.B., 1984, *Geohydrology of the High Plains aquifer in parts of Colorado, Kansas, Nebraska, New Mexico, Oklahoma, South Dakota, Texas, and Wyoming*: U.S. Geological Survey Professional Paper 1400-B, 63 p.) The original data was not supposed to be used at scales larger than 1:1,000,000.

Online linkage: <http://water.usgs.gov/lookup/getspatial?ofr98-414>

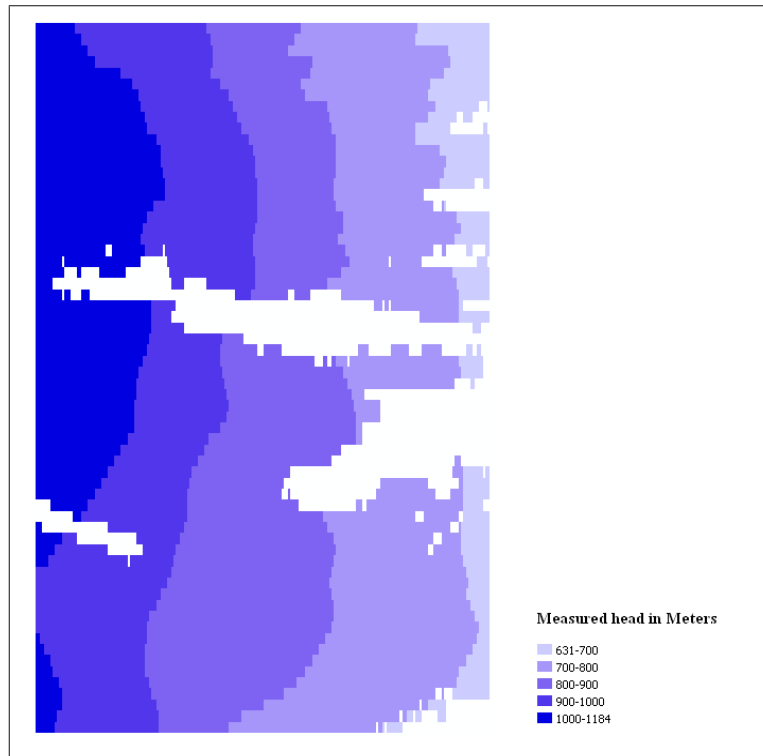


**Figure C.3:** *Predevelopment water level*

This data set consists of digital predevelopment water-level elevation rectangles for the portion of Ogallala Aquifer used in this study. It is a modified version of the digital data set for predevelopment water-level elevations for the High Plains aquifer in the central United States. The original digital data set was created by digitizing the contours for predevelopment water-level elevations from a 1:1,000,000 base map created by the U.S. Geological Survey High Plains RASA project (Gutentag, E.D., Heimes, F.J., Krothe, N.C., Luckey, R.R., and Weeks, J.B., 1984, *Geohydrology of the High Plains aquifer in parts of Colorado, Kansas, Nebraska, New Mexico, Oklahoma, South Dakota, Texas, and Wyoming*: U.S. Geological Survey Professional Paper 1400-B, 63 p.) The original data was not supposed to be used at scales larger than 1:1,000,000.

Online linkage: <http://water.usgs.gov/lookup/getspatial?ofr99-264>

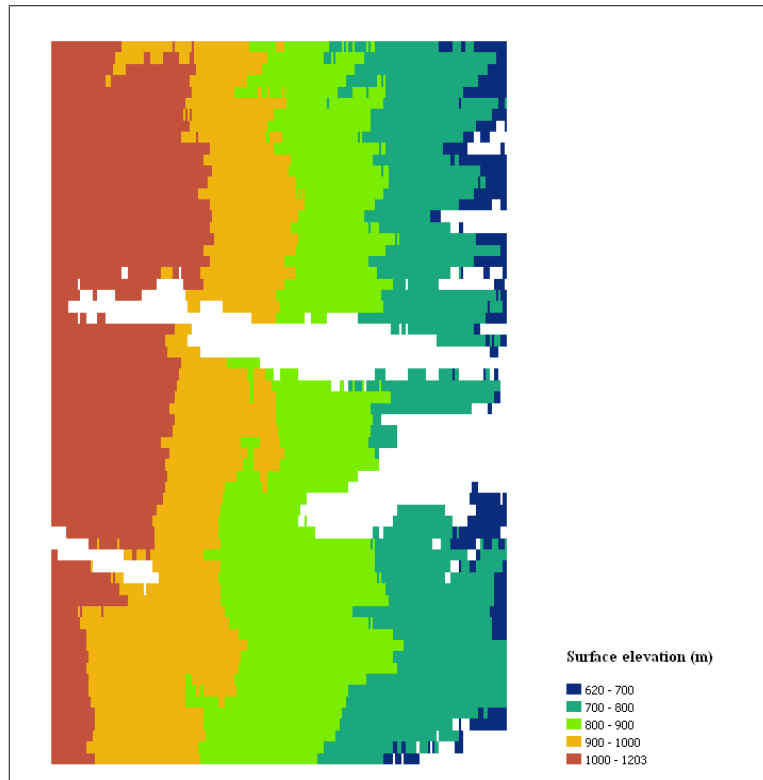


**Figure C.4:** *Surface elevation*

This data set consists of digital surface elevation rectangles for the portion of Ogallala Aquifer used in this study. It is a modified version of the data set for the 2 meter interval LIDAR digital elevation model (DEM) in Kansas, central United States. The original data set was created by U.S. Geological Survey in 2006.

Online linkage: <http://www.kansasgis.org/catalog/catalog.cfm>

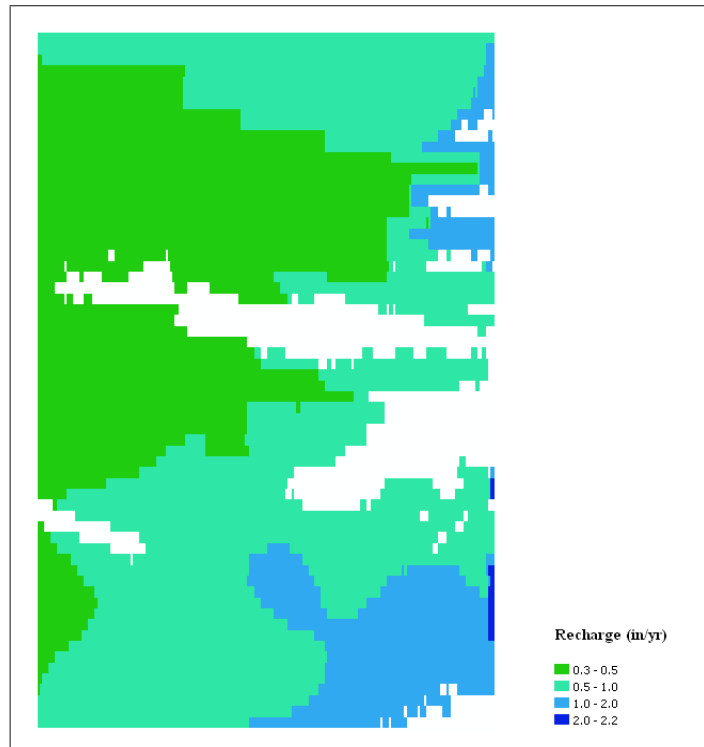


**Figure C.5:** *Annual potential recharge*

This data set consists of digital annual potential recharge rectangles for the portion of Ogallala Aquifer used in this study. It is a modified version of the digital data set for mean annual potential natural recharge in Kansas, central United States. The original digital data set was created by digitizing the contours for mean annual potential natural recharge in Kansas from a 1:500,000 base map created in 1987 by Cristi V. Hansen, U.S. Geological Survey. (Hansen, C.V., 1991, Estimates of freshwater storage and potential natural recharge for principal aquifers in Kansas. Water-Resources Investigations Report 87-4230, USGS, Reston, Virginia, 100 pp)

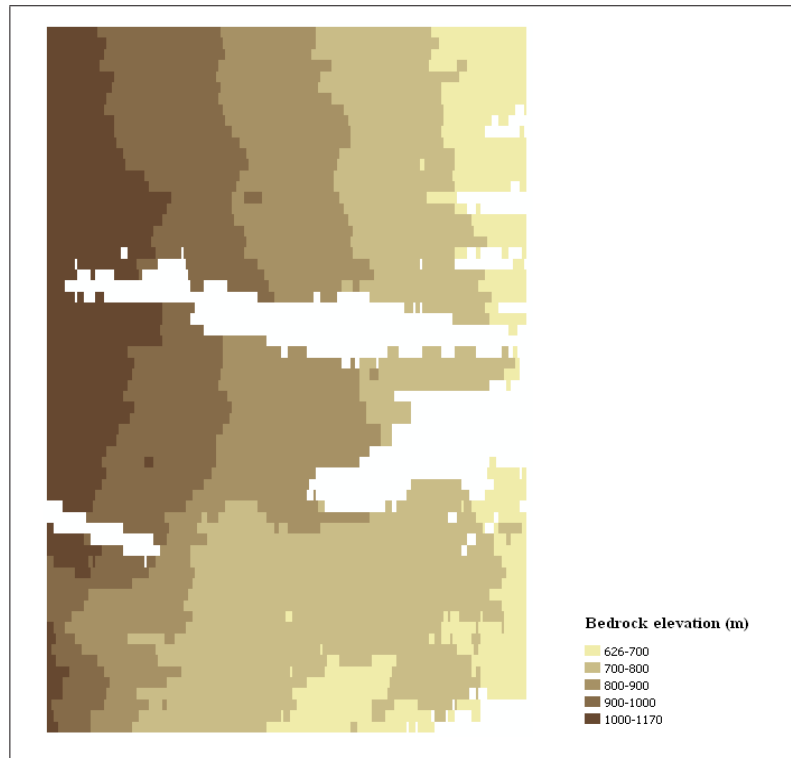


**Figure C.6:** *Bedrock elevation*

This data set consists of digital bedrock elevation rectangles for the portion of Ogallala Aquifer used in this study. It is a modified version of the digital data set for the base of aquifer elevation contours for the High Plains aquifer in the central United States. The original digital data set was created by digitizing the base of aquifer elevation contours from a 1:1,000,000 base map created by the U.S. Geological Survey High Plains RASA project (Gutentag, E.D., Heimes, F.J., Krothe, N.C., Luckey, R.R., and Weeks, J.B., 1984, Geohydrology of the High Plains aquifer in parts of Colorado, Kansas, Nebraska, New Mexico, Oklahoma, South Dakota, Texas, and Wyoming: U.S. Geological Survey Professional Paper 1400-B, 63 p.) The original data was not supposed to be used at scales larger than 1:1,000,000.

Online linkage: [http://water.usgs.gov/lookup/getspatial?ofr98-393\\_aqbase](http://water.usgs.gov/lookup/getspatial?ofr98-393_aqbase)